T.C.

ANTALYA BİLİM UNIVERSITY

INSTITUTE OF POSTGRADUATE EDUCATION

ELECTRICAL AND COMPUTER ENGINEERING

THESIS PROGRAM

COMPARATIVE STUDY OF PI AND MODEL PREDICTIVE CONTROL OF THE DUAL ACTIVE BRIDGE DC-DC CONVERTER

DISSERTATION

PREPARED BY

GILLES AUDRY BAYINA LOUZOLO

ANTALYA – 2022

T.C.

ANTALYA BİLİM UNIVERSITY

INSTITUTE OF POSTGRADUATE EDUCATION

ELECTRICAL AND COMPUTER ENGINEERING

THESIS PROGRAM

COMPARATIVE STUDY OF PI AND MODEL PREDICTIVE CONTROL OF THE DUAL ACTIVE BRIDGE DC-DC CONVERTER

DISSERTATION

PREPARED BY

GILLES AUDRY BAYINA LOUZOLO

ADVISOR

ASST. PROF. DR. MUSTAFA İLKER BEYAZ

ANTALYA – 2022

APPROVAL/NOTIFICATION FORM
ANTALYA BİLİM UNIVERSİTY
INSTITUTE OF POST-GRADUATE EDUCATION

Gilles Audry BAYINA LOUZOLO, a M.Sc. student of Antalya Bılım University, Institute of Post Graduate Education, Electrical and Computer Engineering owning student ID191322016, successfully defended the thesis/dissertation entitled "COMPARATIVE STUDY OF PI AND MODEL PREDICTIVE CONTROL OF THE DUAL ACTIVE BRIDGE DC-DC CONVERTER", which he prepared after fulfilling the requirements specified in the associated legislations, before the jury whose signatures are below.

Academic Tittle, Name-Surname, Signature

Jury Member (Chairman) **:** Asst. Prof.……..…

Jury Member **:** Asst. Prof. Dr. ……..

Jury Member : Asst. Prof.Dr. ……...

Director of the Institute : Prof. Dr. İbrahim Sani Mert

Date of Submission : …/…/2022

Date of Defense : …/…/2022

PREFACE

This Thesis is dedicated to my parents, teachers, and all my friends who have always encouraged me from near and far. I would like to thank my advisors Asst. Prof. Dr. Mustafa lker Beyaz and Ms. Asst. Prof. Farzaneh Bagheri.

Special thank you to the jury members for letting my defense be an enjoyable moment.

10/06/2022

GILLES AUDRY BAYINA LOUZOLO

ÖZET

ÇİFT AKTİF KÖPRÜ DC-DC KONVERTÖRÜNÜN PI VE MODEL ÖNGÖRÜLÜ KONTROLÜ KARŞILAŞTIRMALI ÇALIŞMASI

Yenilenebilir kaynakların kullanımı, enerjiyi ağa entegre etmek için uygun güç elektroniği gerektirir. Bu amaçla çift yönlü dönüştürücüler temel unsurlar haline gelir. Geçtiğimiz yıllarda, çift yönlü dönüştürücünün belirli bir topolojisi, faydaları nedeniyle araştırmacıların dikkatini çekmiştir: "İkili Aktif Köprü dönüştürücü". Performansını artırmak için bu topolojinin çalışması ve kontrolü kapsamlı bir şekilde incelenmelidir. Bu tezde, sistem çalışması için en iyi kontrol yaklaşımını seçmek için tek yönlü bir güç transferi uygulamasında kullanım için DAB dönüştürücünün PI Kontrolü ve Model Tahminli Kontrolünün karşılaştırmalı bir değerlendirmesi yapılmıştır.

Bu analiz için seçilen metodoloji, sistem çalışmasının üç (3) farklı çalışma senaryosunda araştırılmasıydı: kararlı durum, dinamik yanıt ve giriş voltajı değişikliği (bozulma). Tahmini voltaj kontrol yaklaşımı, MATLAB'da simülasyon için bir S-Fonksiyonu olarak geliştirilmiştir.

ABSTRACT

COMPARATIVE STUDY OF PI AND MODEL PREDICTIVE CONTROL OF THE DUAL ACTIVE BRIDGE DC-DC CONVERTER

The use of renewable sources requires suitable power electronics for integrating energy into the network. For this purpose, bidirectional converters become essential elements. Over the past years, a particular topology of bidirectional converter has attracted the attention of researchers due to its benefits: “The Dual Active Bridge converter”. The operation and control of this topology must be thoroughly studied to increase its performance. In this thesis, a comparative evaluation of PI Control and Model Predictive Control of the DAB converter for use in a unidirectional power transfer application was conducted to choose the best control approach for the system operation.

The methodology chosen for this analysis was the investigation of the system operation in three (3) different working scenarios: the steady-state, the dynamic response, and the input voltage change (disturbance). The predictive voltage control approach was developed as an S-Function for simulation in MATLAB.

Keywords: DAB, MPC, PI, SPS, Dual Active Bridge

TABLE OF CONTENTS

PREFACE ..... **iii**

ÖZET ..... **iv**

ABSTRACT ..... **v**

LIST OF TABLES ..... **ix**

LIST OF FIGURES ..... **x**

LIST OF ABBREVATIONS ..... **xii**

CHAPTER 1 INTRODUCTION **1**

1.1 Problem Background **1**

1.2 Methodology **2**

1.3 Thesis Outline **3**

CHAPTER 2 LITERATURE REVIEW **4**

2.1 Converter Selection **5**

2.1.1 Flyback Converter **6**

2.1.2 Current Fed Push-pull Converters **7**

2.1.3 Bridge Converters **9**

2.1.3.1 Half-Bridge Converter ***9***

2.1.3.2 Full-Bridge Converter ***10***

2.2 Modulation Techniques **11**

2.2.1 Single Phase Shift Modulation (SPS) Technique **12**

2.2.2 Triangular Modulation (TRM) Technique **13**

2.2.3 Extended Single-Phase Shift (ESPS) Technique **14**

2.3 Electrical Network Topology and Principle **15**

2.4 Different Applications of the DAB **15**

2.4.1 Automotive: **16**

2.4.2 Renewable Energy: **16**

2.4.3 Smart Grid: 16

CHAPTER 3 DAB CONVERTER 17

3.1 Single Phase DAB 18

3.2 Steady-State Analysis 19

3.3 DAB Parameters 21

3.4 Mathematical Model of the DAB (Using SPS) 22

3.4.1 Dynamic Equations of the DAB 22

3.4.2 Transfer Function of the DAB 24

CHAPTER 4 CONTROL METHODS OF THE DAB 27

4.1 PI CONTROL 28

4.1.1 PI Transfer Function 29

4.2 Model Predictive Control of the DAB Converter 30

4.2.1 Basics of MPC 31

4.2.2 Predictive Control of the Single-Phase DAB 33

4.2.3 Control Strategy of the DAB Using MPC 34

4.2.4 Model of the DAB Converter Supplying a Load R 34

4.2.4.1 Reduced Order Model 34

4.2.4.2 Discrete-Time Model 35

4.2.5 Cost Function 36

4.2.6 Moving Discretized Control Set MPC of DAB Converter 36

4.2.9 Cost Function Proposed 38

CHAPTER 5 SIMULATIONS RESULTS 39

5.1 PI Control of DAB converter 40

5.1.1 Voltage waveform 41

5.1.2 Simulation Results: Stable Load R 42

5.1.3 Simulation Results: Variation in the Load (Dynamic Response) 42

5.1.4 Simulation Results: Variation in Vin (Disturbance) 44

5.2 MPC Control of DAB converter 45

5.2.1 Voltage Waveform 46

5.2.2 Simulation Results: Stable Load R 47

5.2.3 Simulation Results: Variation in the Load (Dynamic Response) 47

5.2.4 Simulation Results: Variation in Vin (Disturbance) 48

5.2.5 Cost Function 49

5.3 Comparison Between the PI and MPC 49

CHAPTER 6 CONCLUSION AND WORK TO BE DONE IN THE FUTURE 51

6.1 Conclusion 51

6.2 Future Work 51

REFERENCES 52

Appendix 1: MATLAB PLOTS WITH PI CONTROLLER 55

Appendix 2: MATLAB PLOTS WITH MPC 56

LIST OF TABLES

Table 1: Parameters in operation 22
Table 2: Operating parameters for simulation 39
Table 3: Comparison of PI and MPC at Stable Load..... 49
Table 4: Comparison of PI and MPC with Step change in the load at t=0.5 seconds ... 50
Table 5: Comparison of PI and MPC with Step change in the input voltage 50

LIST OF FIGURES

Figure 1: Typical Structure of a non-isolated type of converter 4
Figure 2: Typical Structure of a non-isolated Converter 5
Figure 3: Simple structure of a unidirectional flyback converter 6
Figure 4: Waveforms generated by a unidirectional Flyback Converter 6
Figure 5: Structure of a bidirectional flyback converter 7
Figure 6: Unidirectional fed push-pull converter 7
Figure 7: Waveforms generated by a current fed Push-pull Converter 8
Figure 8: Bidirectional fed push-pull converter 8
Figure 9: Unidirectional Structure of a half-bridge converter 9
Figure 10: Half-Bridge Converter waveform 10
Figure 11: Bidirectional Structure of a half-bridge converter 10
Figure 12: Structure of the single-phase DAB 11
Figure 13: Structure of the three-phase DAB 11
Figure 14: Single Phase Shift Modulation: waveforms 12
Figure 15: Triangular Modulation waveforms 13
Figure 16: ESPS Modulation: Waveforms 14
Figure 17: Network topology 15
Figure 18: Circuit of the Single-Phase DAB converter 18
Figure 19: Simplified equivalent circuit of the DAB 20
Figure 20: Waveform of operating mode 20
Figure 21: Basic structure of a closed loop control 28
Figure 22: PI Controller Structure 29
Figure 23: Predictive control approaches (Cortes et al., 2008 © IEEE) 31
Figure 24: Basic Structure of MPC 32
Figure 25: MPC Strategy 33
Figure 26: DAB model average [12] 34
Figure 27: Predictive Voltage control block diagram 36
Figure 28: Operating principle of the MPC for DAB [12] 37
Figure 29: Circuit diagram of the PI control of the DAB converter 40
Figure 30: SPS voltage waveforms 41
Figure 31: Output voltage and Output Current 42

Figure 32: Step change of the load 42
Figure 33: Variable load 43
Figure 34: Change in the input Voltage (Disturbance) 44
Figure 35: Circuit diagram of the MPC of the DAB converter 45
Figure 36: Pulses generator for the switches 45
Figure 37: Block containing the control algorithm 46
Figure 38: SPS voltage waveforms 46
Figure 39: Output voltage and Output Current 47
Figure 40: Step change of the load 47
Figure 41: Step change of the input Voltage (Disturbance) 48
Figure 42: Cost function 49

LIST OF ABBREVATIONS

PSM	: Phase Shift Modulation
SPS	: Single-Phase Shift Modulation
ESPS	**:** Extended Single-Phase Shift Modulation
DPS	: Dual-Phase Shift Modulation
TPS	: Triple-Phase Shift Modulation
DAB	: Dual-Active-Bridge
TPZM	: Trapezoidal Modulation
PI	: Proportion-Integral
MPC	: Model Predictive Control
BDC	: Bidirectional Converter

CHAPTER 1
INTRODUCTION

1.1 Problem Background

Traditional energy sources, such as coal, oil, and other resources of fossil fuels, have been heavily exploited by humans over the course of the past two centuries. Electrical energy has always been one of the most essential sources of energy, and it will continue to be in the foreseeable future. It has been a driving force behind the industrialization and expansion of economies all over the world. According to the findings of the Intergovernmental Panel on Climate Change (IPCC), the generation of electrical energy is responsible for 37 percent of global emissions. By substituting renewable energy sources for existing polluting energy sources, this emission rate can be lowered (World Nucl. Assoc., p.10, 2011.). Considering this, the need for energy with little environmental impact is growing.

However, the biggest problem with renewable energies is intermittency. Most renewable energy sources are heavily dependent on daily weather conditions. They are unable to provide constant output power resulting in the possibility of not always meeting the grid power demand. Power electronic systems, such as bidirectional converters (Zeng, Jianwu, Du, Xia, Yang and Zhaoxia. (2021)), need to be introduced as a link point between energy storage, sources of energy, and the grid to regulate the flow of power.

Nevertheless, the Bidirectional converter itself needs to be controlled to be efficient. The focus of this thesis will therefore be on the control of the Single-Phase DAB converter, which is the most popular topology of bidirectional converter. A specific control scheme called Model Predictive Control is introduced and simulated. The results are compared to the common PI control method. All simulations are performed using the Software MATLAB.

1.2 Methodology

First, the characteristics of the DAB are selected: the leakage inductance L_r, the output capacitor C_o and the input Voltage V_{in}. Because every switch is presumed to be perfect, the losses are not taken into account.

This thesis only takes into consideration the unidirectionality of the dual active bridge, meaning that the converter works in buck mode. The load is a resistive charge R, and the frequency is constant f_{sw}. For the mathematical model, a reduced-order representation of the DAB served as basis.

The DAB's output voltage is regulated by a moving discretized control set (MPC), and the Single-Phase Shift is the modulation technique utilized to generate the necessary voltages. In the first part, the DAB is controlled using the PI controller then in the second part, the DAB is controlled using the MPC.

In MATLAB, the predictive voltage control approach is implemented as an S-Function for simulation. The MATLAB function integrates the algorithm required to determine the most effective control action for driving the output voltage to the reference.

Different working operations are considered:

- The steady-state
- The dynamic response
- The change in the input voltage: Assuming a disturbance

The results of the simulation under these three (3) scenarios are analyzed and compared then the best control method is determined.

1.3 Thesis Outline

The DAB converter is discussed in length in the three first chapters in terms of its overall introduction, control techniques, transmission power characterization, and topologies. Chapter 4 presents the design of the control methods: The PI and the MPC. Chapter 5 presents the simulation model as well as the simulation results of the PI and MPC control of the DAB. In Chapter 6, the conclusion and future work to be done are presented.

CHAPTER 2
LITERATURE REVIEW

Different topologies of bidirectional converters have been introduced in the literature. Over the course of the past three decades, these converters have been the subject of a great amount of study attention, which has led to the development of many written documents.

In order to effectively handle a large number of articles and evaluate their contributions, the published contents can be separated into two main categories:

- Topology selection
- Modulation technique

A bidirectional converter is a converter allowing the power to flow forward and backward. A BDC comes in a variety of designs and can be classified into two groups: the non-isolated type (Figure 1) and the isolated type (Figure 2). Each application has a corresponding type of bidirectional converter according to the needs.

- Where size, weight, price are parameters of choice and a wide conversion voltage range is not required, the non-isolated bidirectional type is preferable. Figure 1 depicts the non-isolated type of bidirectional converter structure; there is a physical connection between the input and the output side.

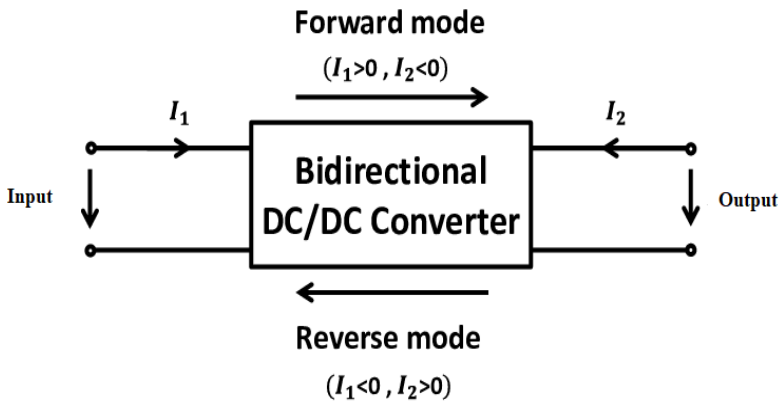

Figure 1: Typical Structure of a non-isolated type of converter

- Where a large conversion ratio and galvanic isolation are required for safety purposes (such as Microgrid application), isolated bidirectional converters are preferable. Unlike non-isolated converters, they are more complicated and expensive, but they improve the safety and reliability of the system besides realizing the smooth switching function by applying the phase shift control. Figure 2 depicts the structure of an isolated bidirectional converter. The two bridges are separated by a transformer.

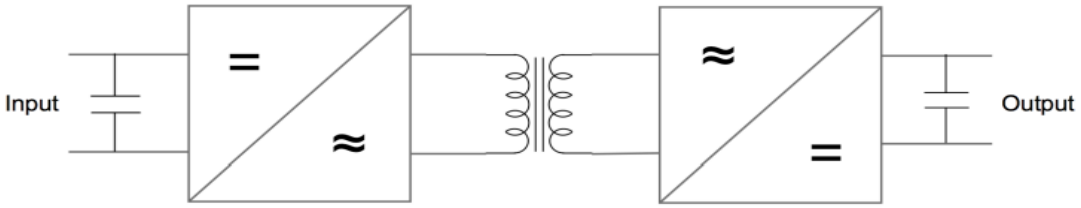

Figure 2: Typical Structure of a non-isolated Converter

The BDC controls the power transfer which occurs from V_1 (DC Voltage Source) to V_2 (DC Voltage load). The converter can operate in two different modes:

- In forward mode (+), the power is transmitted from Vin to Vout.
- During operation in the reverse mode, the power flows from Vout to Vin.

2.1 Converter Selection

Major bidirectional topologies include the following:

- Current Fed Push-pull Converters
- Flyback Converters
- Bridge Converters

2.1.1 Flyback Converter

The flyback converter's structure is depicted in Figure 3. This converter is popular due to its low number of components. In this converter, the output filter inductors are not essential. One benefit of this converter is its capability of providing multiple voltage values by utilizing a transformer containing numerous output windings.

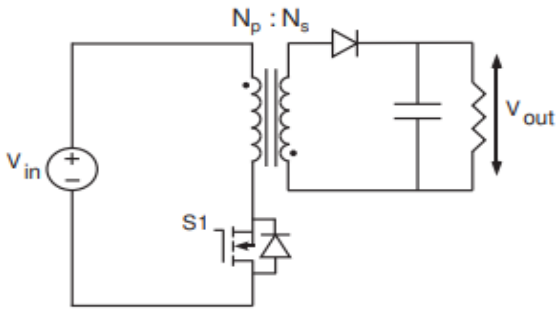

Figure 3: Simple structure of a unidirectional flyback converter

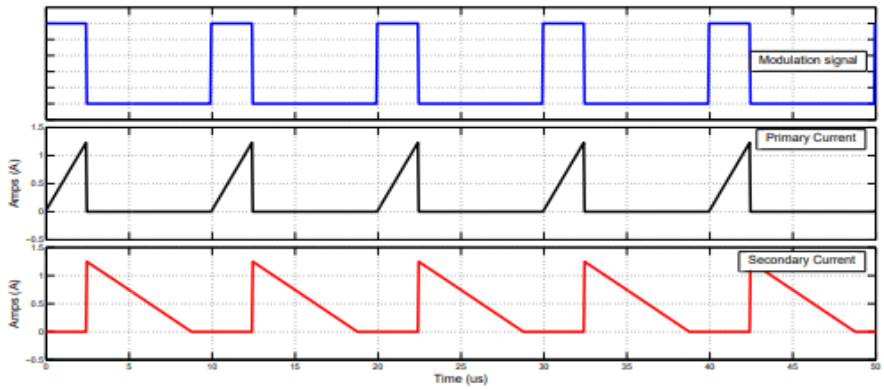

Figure 4: Waveforms generated by a unidirectional Flyback Converter

Note: Image from "Dynamic Modelling and Control of Dual Active Bridge Bi-directional DC-DC Converters for Smart Grid Applications", by Dinesh Sekhar Segaran, 2006, p10

As the structure represented in Figure 3 has a unidirectional nature, to make it bidirectional it is necessary to connect an additional similar converter at the second side of the transformer (Gang, C., Yim-Shu, L., Hui, S.Y.R., Xu, D. and Wang, Y. (2000)).

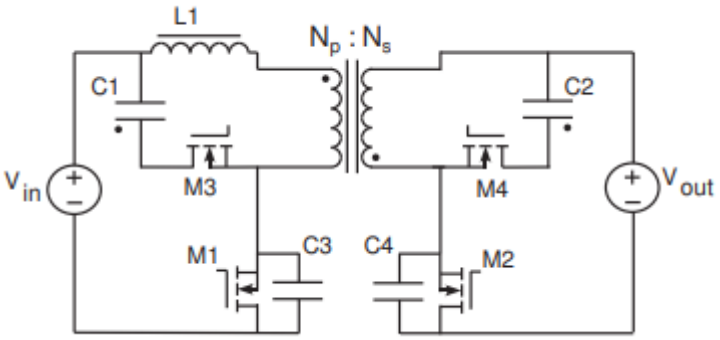

Figure 5: Structure of a bidirectional flyback converter

Figure 5 shows the structure of an actively clamped bidirectional flyback converter. The bidirectional flow of power is obtained by controlling the switches according to the power flow direction needed. One disadvantage of the Flyback converters is the fact that they are only appealing at relatively low levels of voltage and power (Gang, C., Yim-Shu, L., Hui, S.Y.R., Xu, D. and Wang, Y. (2000)).

2.1.2 Current Fed Push-pull Converters

The unidirectional Current fed Push-pull Converter Topology is depicted in Figure 6. Simple in configuration and offering high power-to-weight ratio, this switch mode power supply topology is widely used.

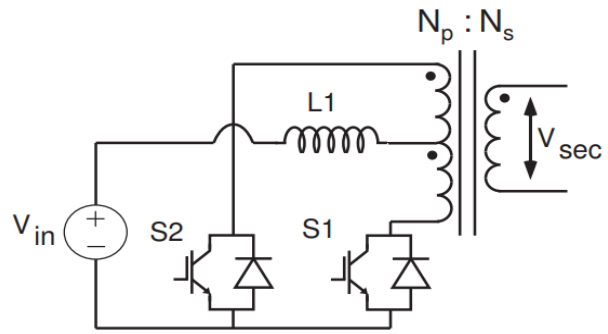

Figure 6: Unidirectional fed push-pull converter

Figure 7 shows the converter's operation. When only the switch S1 is ON, V_{sec} has a positive value and when only the switch S2 is ON, V_{sec} is negative.

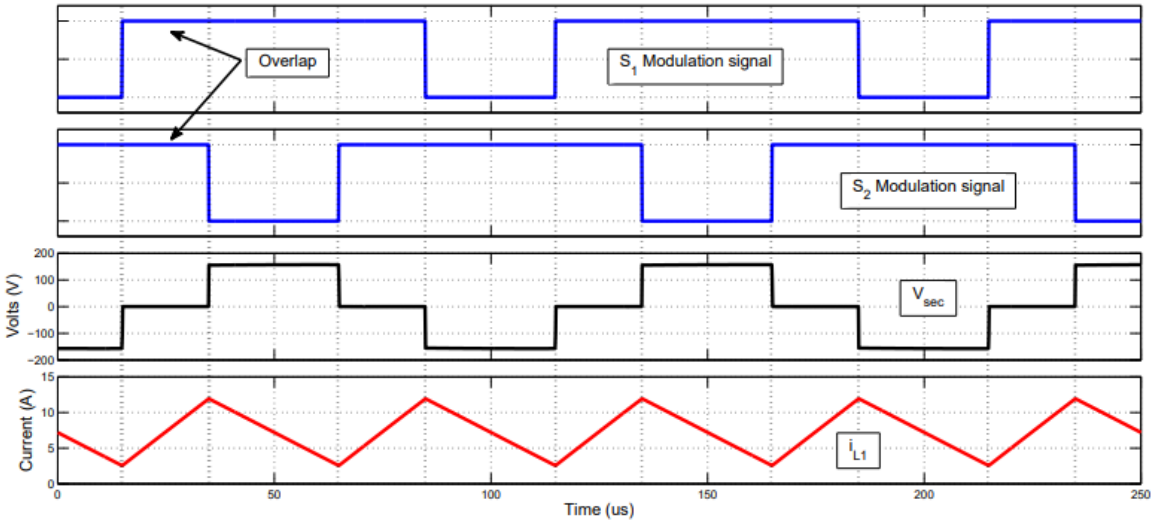

Figure 7: Waveforms generated by a current fed Push-pull Converter

Note: Image from "Dynamic Modelling and Control of Dual Active Bridge Bi-directional DC-DC Converters for Smart Grid Applications", by Dinesh Sekhar Segaran, 2006, p12

To obtain bidirectional power flow, another converter needs to be linked at the secondary side of the transformer. This additional converter is not required to be another push-pull converter. Figure 8 depicts the structure of a bidirectional fed push-pull converter. In this structure, a half-bridge is connected to the transformer (Cacciato, M., Caricchi, F., Giuhlii, F. and Santini, E. (2004)).

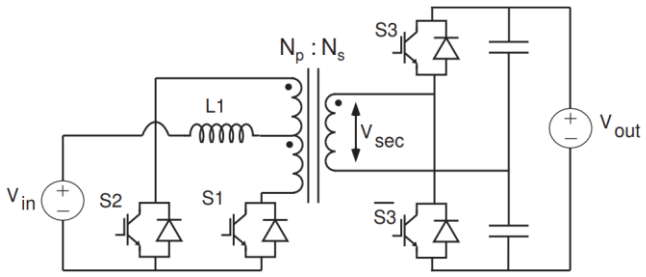

Figure 8: Bidirectional fed push-pull converter

2.1.3 Bridge Converters

The bridge converter is by far the most common type of isolated bidirectional converter used due to its advantages: bidirectionality in power flow and high-power density (R. W. A. A., De Doncker, Divan, D.M. and Kheraluwala, M. H. (1993)). Bridge converters are built with phase legs. Each of them is equipped with switches that can be controlled according to the level of voltages desired.

Two types of bridge converters can be classified:

- Half-bridge

- Full-Bridge

2.1.3.1 Half-Bridge Converter

A Half-bridge is made up of a parallel single-phase leg.

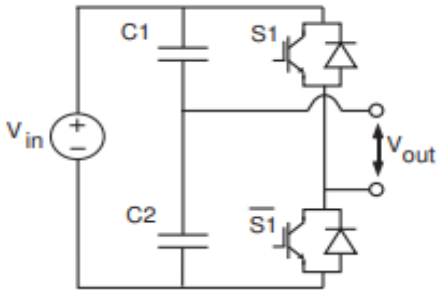

Figure 9: Unidirectional Structure of a half-bridge converter

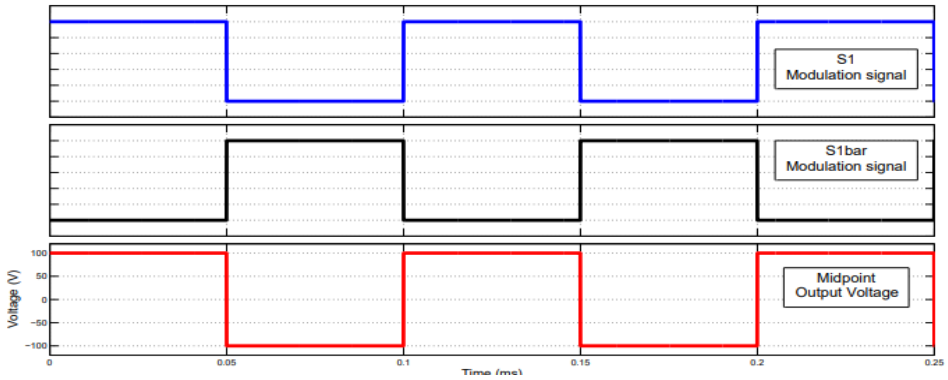

Figure 10: Half-Bridge Converter waveform

Note: Image from "Dynamic Modelling and Control of Dual Active Bridge Bi-directional DC-DC Converters for Smart Grid Applications", by Dinesh Sekhar Segaran, 2006, p14

To obtain a bidirectional half-bridge converter, an additional half-bridge needs to be connected at the secondary side of the transformer.

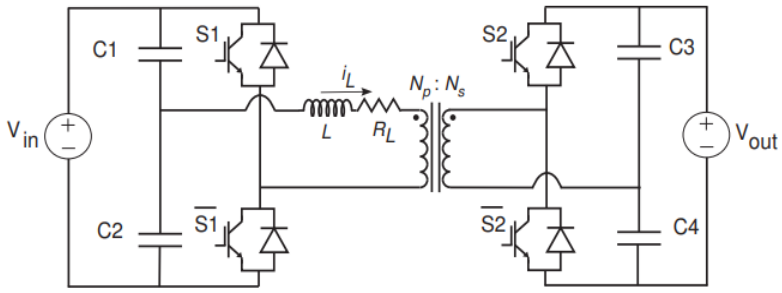

Figure 11: Bidirectional Structure of a half-bridge converter

2.1.3.2 Full-Bridge Converter

Depending on the configuration, a Full-bridge converter might have two or three legs. The following are the most common types of full-bridge converters:

- The Single-Phase H-Bridge

- The Three-Phase Bridge

In contrast to the Half-Bridge converter, the DAB converters are made up of several switches (the single-phase bridge counts 8 switches, and the three-phase bridge counts 12 switches).

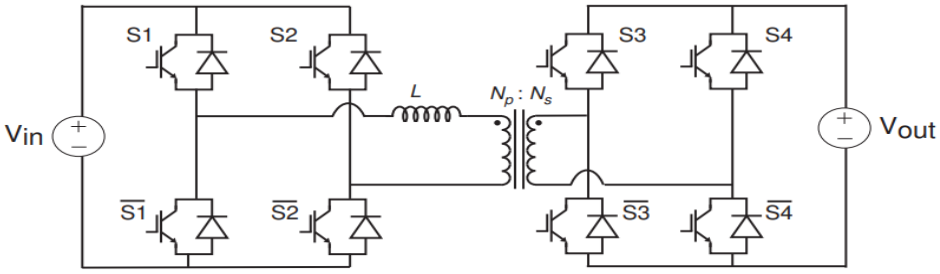

Figure 12: Structure of the single-phase DAB

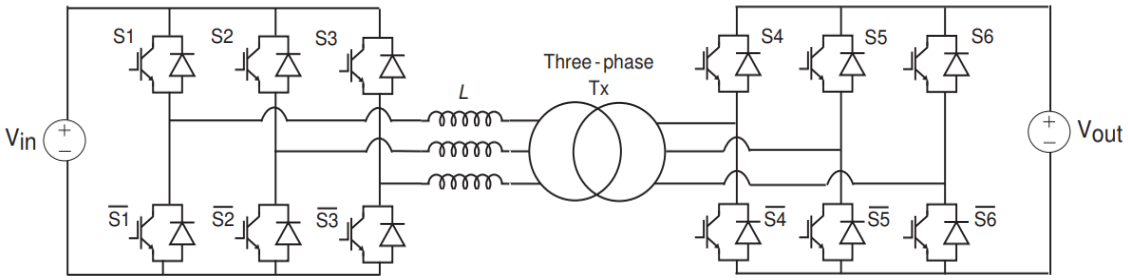

Figure 13: Structure of the three-phase DAB

Note: Images from "Dynamic Modelling and Control of Dual Active Bridge Bi-directional DC-DC Converters for Smart Grid Applications", by Dinesh Sekhar Segaran, 2006, p16

2.2 Modulation Techniques

Some modulation techniques that have been applied to the full-bridge in the research are going to be discussed in this section, along with a summary of their important characteristics. To manage the flow of power efficiently in a DAB converter, an efficient modulation is necessary. The common modulation techniques are:

- The Single-Phase Shift (SPS),
- The Triangular Modulation (TRM)

- The Extended Single-Phase Shift (ESPS)

2.2.1 Single Phase Shift Modulation (SPS) Technique

This modulation technique is used for higher power transfer. The main idea behind this modulation method is the control of the power transmitted based on the phase shift existing between the bridges. In this thesis, the unidirectional power transfer is considered. The primary bridge transmits power to the secondary bridge. This technique uses a fixed duty ratio D = 0.5.

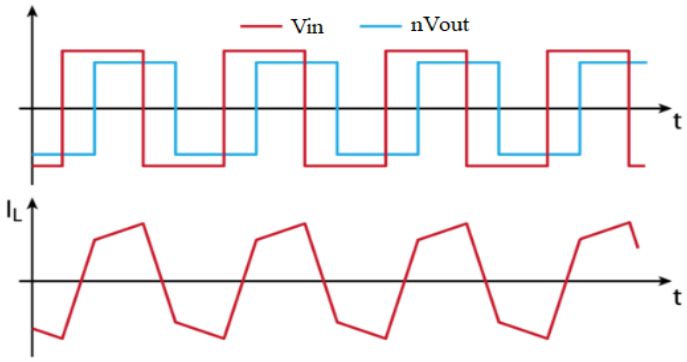

Figure 14: Single Phase Shift Modulation: waveforms

Figure 14 illustrates the waveforms of both the switching voltage and the inductor current. The power transmitted is positive and can be expressed as:

$$P = \frac{V_{in} V_{out}}{L_r f_{sw}} \phi(1-2\phi) \quad (1)$$ as the turn ratio of the transformer is 1 (Lucas, Kevin, Pagano, Daniel, Landau. and Renan. (2019))

The voltage at the input is V_{in}

The voltage at the output is V_{out}

The leakage inductance is L_r

ϕ denotes the phase shift

The output voltage is relatpaed to the phase shift, its value will vary accordingly during the system's operation.

2.2.2 Triangular Modulation (TRM) Technique

The use of triangular modulation is presented in (Yade, Ousseynou, Gauthier, Jean-Yves, lin shi, Xuefang, Gendrin, Martin, Zaoui and Abderrahim. (2015).), and a subsequent study reveals that this technique is well suited for the transfer of low powers in a DAB converter. Both duty ratio of the first bridge voltage d_1 and the duty ratio of the first bridge d_2 can be utilized to regulate the flow of power.

The power transfer can be expressed as:

$$P = \frac{V_{in}^{2} * d_1^{2}}{L_r f_{sw}} \qquad (2)$$

The duty ratio is expressed as:

$$d_1 = \frac{\sqrt{P * L_r * f_{sw}}}{V_{in}} \qquad (3)$$

$$d_2 = d_1 \frac{n * V_{in}}{V_{out}} \qquad (4)$$

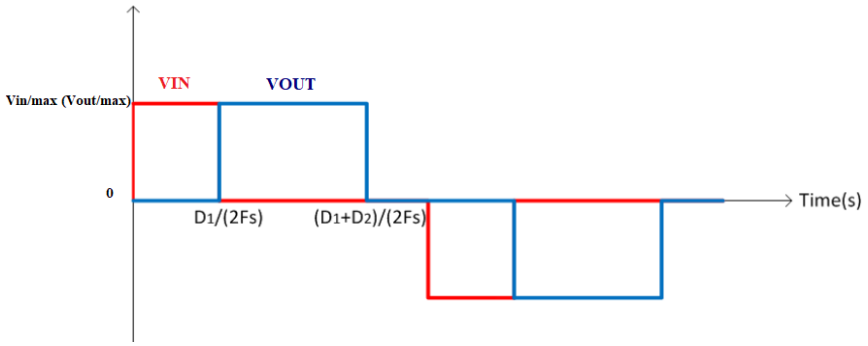

Figure 15: Triangular Modulation waveforms

Note: Image from Yade, Ousseynou, Gauthier, Jean-Yves, lin shi, Xuefang, Gendrin, Martin, Zaoui and Abderrahim. (2015), p2

2.2.3 Extended Single-Phase Shift (ESPS) Technique

The use of the ESPS technique is introduced in (Shi, X., Jiang, J. and Guo, X. (2012)). It incorporates both SPS and TRM modulation. Two modes of operation are achievable: In mode one, the first bridge applies the TRM modulation as depicted in Figure16, while the second bridge applies the SPS. In mode two, on the other hand, the situation is reversed.

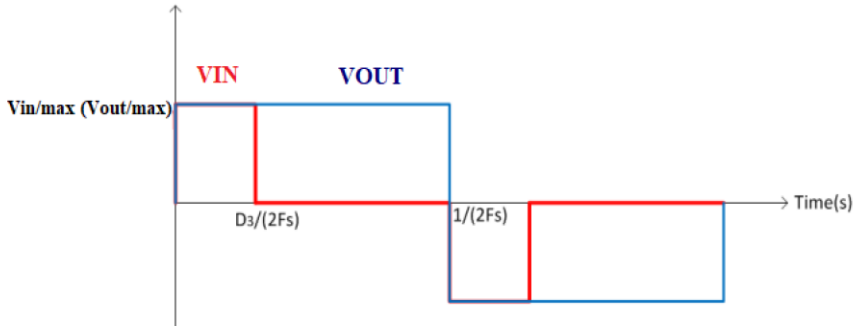

Figure 16: ESPS Modulation: Waveforms

Note: Image from Yade, Ousseynou, Gauthier, Jean-Yves, lin shi, Xuefang, Gendrin, Martin, Zaoui and Abderrahim. (2015), p2

In both modes the power transfer is similar and can be expressed as:

$$P = \frac{V_{in} * V_{out}}{4nL_r f_{sw}} d_3(1 - d_3) \qquad (5)$$

The TRM's duty ratio is denoted by the symbol d_3 and can be expressed as:

$$d_3 = \frac{1}{2}\left(1 - \sqrt{1 - \frac{16 * |P| nL_r 2f_{sw}}{V_{in} * V_{out}}}\right) \qquad (6)$$

2.3 Electrical Network Topology and Principle

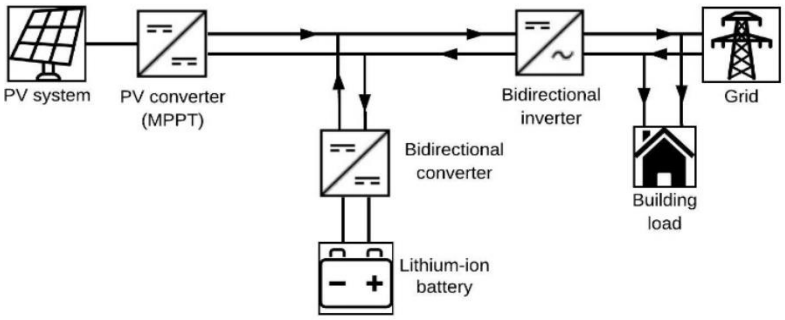

Figure 17: Network topology

In the electrical network shown in Figure 17, the battery can be fed from both systems: the cells and the grid through a BDC. When the PV system cannot provide enough output power to the grid at night or on a cloudy day for example, the battery discharges its stored energy through the BDC.

In fact, the grid can take different forms in certain cases. It can either behave as a passive or an active component. When the grid behaves as a passive component, it takes power from the system. When the grid behaves as an active component; it supplies the power to the rest of the system. The Bidirectional Converter is considered a key device for interfacing the battery, the PV array, and the grid for continuous flow of power. In the thesis application, the load is passive, so it receives the power from the battery located at the input side.

2.4 Different Applications of the DAB

DAB converters are utilized in a variety of applications due to the numerous benefits that they offer. They lower the number of components because the output inductor filter is not necessary in their design. The zero-voltage switching (ZVS) is feasible and does not require the addition of any components. By modifying the transformer’s turn ratio, they have the option to step up or step down the voltage as needed.

Either a transformer or capacitors can provide the necessary galvanic isolation for a circuit. Furthermore, they reduce the amount of voltage stress across the switches. In addition to this, high power densities are accomplished while maintaining a high degree of efficiency. On the other hand, one of the drawbacks of DAB is the existence of a high circulating current in the transformer, which results in an increase in losses and causes the converter to lose its ability to switch at zero voltage when the load is light (R. W. A. A., De Doncker, Divan, D.M. and Kheraluwala, M. H. (1993)).

2.4.1 Automotive:

Reduced fuel consumption is currently a popular topic of discussion in the automotive industry as a whole. There is currently a push toward the commercialization of hybrid electric cars (HEV), electric vehicles (EV), and fuel cell vehicles. DAB converters are being utilized in vehicle technologies due to its high efficiency, high power density, and low weight (Krismer, F. and Kolar, J.W. (2010)).

2.4.2 Renewable Energy:

DAB converters serve as a link point between energy storage, sources of energy, and the grid to control the power transfer. Hence, they are considered as fundamentals in renewable energy applications. (Tsai, M.T., Chu, C.L., Yang, Y.Z. and Wu, D. R. (2016).)

2.4.3 Smart Grid:

Connecting variable sources and storage systems to the Smart Grid is a challenging task due to the differences in voltages, frequency, and magnitude (Barone, G., Brusco, G., Burgio, A., Menniti, D., Pinnarelli, A. and Sorrentino, N. (2014)). This is in addition to the task of controlling the power flow direction, which is especially challenging during fluctuations. Alternating Current (AC) is used by the Smart Grid, whilst Direct Current (DC) is used by the sources and the storage system (DC). Therefore, converters are utilized to interface these two different forms of voltages and currents and to regulate the flow of power during both steady-state and transient conditions.

CHAPTER 3
DAB CONVERTER

In this chapter, the DAB converter is discussed. The single-phase DAB converter is the subject of this thesis. In (Zhao, B., Song, Q., Liu, W. and Sun, Y. (2014)) and (Naayagi, R., Forsyth, A.J. and Shuttleworth, R. (2012)), the results of an investigation into the design, the operation, and the control of the DAB converter are presented. In high frequencies, it has been demonstrated that the phase shift and the leakage inductance are the main parameters to be considered for the power transfer.

To understand the working principle of this converter, a steady-state analysis, and a small-signal model have been done in (Harrye, Y.A., Ahmed, K.H., Adam, G.P. and Aboushady, A.A. (2014)). It has been determined that the capacity of the power transmitted is proportional to the multitude of switches. (Zhao, B., Song, Q., Liu, W. and Sun, Y. (2014)).

There are different types of Dual Active Bridges. The most popular ones are the three-phase and the Single-Phase DAB. The DAB converter was chosen as the topology for this thesis because of its many advantages:

- Simple structure,
- Bidirectional power flow capacity,
- Galvanic isolation,
- Simplicity of single-phase shift implementation.

Moreover, the motivation for this choice is the fact that it uses a low number of passive components. Galvanic isolation is among the most significant benefits offered by the DAB. The isolation protects each side of the converter. For example, in buck mode operation, if there were to be a problem at the Bridge 1 side, Bridge 2 side would not be affected because of the isolation (Abraham, Y.H., Wen, H., Xiao, W. and Khadkikar, V. (2011)).

3.1 Single Phase DAB

A DAB converter is able to transfer power in either the forward or reverse direction. This converter consists of two active bridges physically separated from each other by a transformer. Each active bridge has an H-bridge connection and contains four controllable switching devices. The transformer acts as a means by which each side of the converter can be kept galvanically isolated from the other. It is necessary for the transformer to work at high frequency in order to reduce its weight and size.

The quantity of energy that is transferred is directly proportional to the leakage inductance of the transformer, making it a critical component of the system. Utilizing the output capacitance of switching devices is key for achieving soft-switching operation (Kayaalp, İlker, Demirdelen, Tuğçe, Tümay, and Mehmet. (2016); Doncker, R.D., Divan, D. and Kheraluwala, M. (1991)). Figure 18 shows the structure of the DAB converter utilized in this thesis.

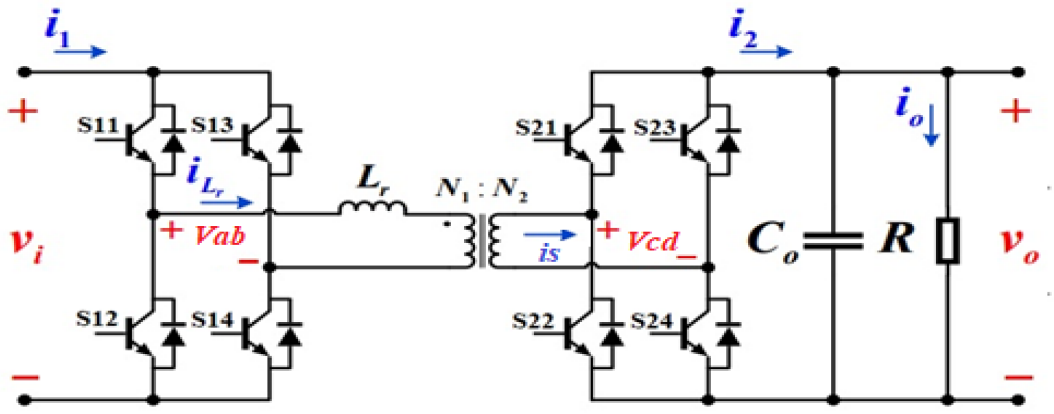

Figure 18: Circuit of the Single-Phase DAB converter

Figure 18 depicts the components that make up the DAB converter's circuit. These components are as follows:

- 1 voltage source
- 1 Capacitor in the output

- 8 MOSFETs
- 1 isolated Transformer
- A leakage inductance L_r
- A load R

This circuit is bidirectional and regulated by a phase shift existing between the bridges. One of the converters converts the DC voltage into an AC waveform, which is subsequently delivered to the transformer, depending on the direction of the power flow (forward or reverse). The other converter then rectifies the AC signal and converts it to DC.

3.2 Steady-State Analysis

Figure 19 shows a simple equivalent DAB converter circuit. To make the analysis easier:

- All resistance is assumed to be zero
- The transformer magnetizing inductance is ignored
- The transformer winding capacitance is ignored
- The frequency is a constant

The equivalent leakage inductance replaces the transformer. The switches operate with a 50% duty ratio, turning on/off diagonally in the same bridge at the same time. The amount of power to be transmitted from one bridge to the other is determined by the phase shift ϕ.

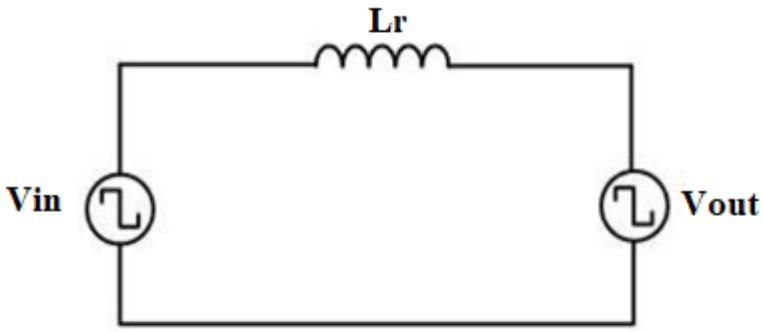

Figure 19: Simplified equivalent circuit of the DAB

The operation in steady states and the converter's operating waveforms are shown in Figure 20. The switching signals of the converters are identical for S11 and S14, which are complementary to S12 and S13.

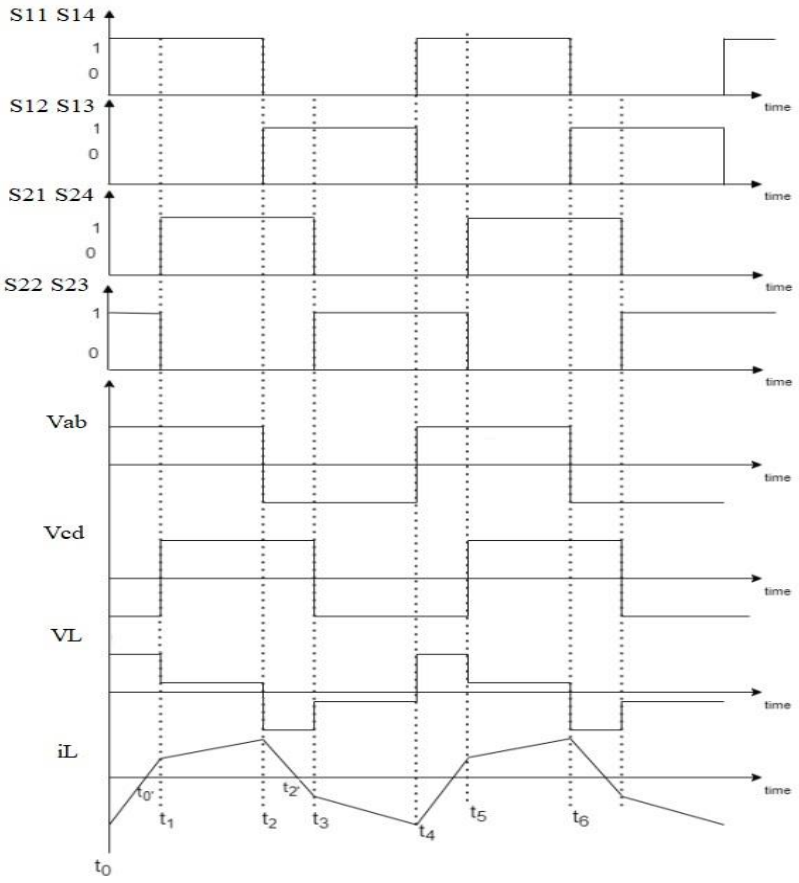

Figure 20: Waveform of operating mode

Figure 20 is a schematic representation of the gating pulses generated by the switches of the circuit. Vab is the voltage on the bridge 1, Vcd is the voltage on the Bridge 2. iL represents the current flowing through the transformer.

3.3 DAB Parameters

Before the simulation of the system, it is necessary to define the different parameters. The transformer turn ratio is assumed to be equal to one throughout the entirety of this thesis. Every switch operates at a set Duty cycle = 0.5. The operating conditions are mentioned in Table 1. The switching frequency is considered constant $f_{sw} = 5kHz$, and the switches are considered ideal with zero commutation time (so instantaneous turn on and off). The leakage inductance is fixed as $L_r = 280\mu H$

$$L_r = \frac{nV_{in}V_{out}}{8f_{sw}P} \qquad (7)$$

$V_{in} = 100V$

$V_{out} = 70V$

$C_0 = 10000\mu F$

From the equation (1), when $\phi = \pm\frac{\pi}{2}$, the maximum power is transferred in the system. $P = 625$ Watts is the maximum power to be transferred with the parameters chosen.

Table 1: Parameters in operation

Parameters	Values
Converter rated power P	625 W
Primary voltage V_{in}	100 V
Secondary Voltage V_{out}	70 V
Transformer turn ration n	1
Power transfer inductance L_r	280 μH
Switching frequency f_{sw}	5 kHz
Load resistor R	20 Ω
Capacitance C_o	10000 μF

3.4 Mathematical Model of the DAB (Using SPS)

3.4.1 Dynamic Equations of the DAB

The DAB converter's switching states are determined by the gating signals, which are as follows:

$$S_a = \begin{cases} 1, S_{11} \text{ is on and } S_{12} \text{ is off} \\ 0, S_{11} \text{ is off and } S_{12} \text{ is on} \end{cases} \quad (8)$$

$$S_b = \begin{cases} 1, S_{13} \text{ is on and } S_{14} \text{ is off} \\ 0, S_{13} \text{ is off and } S_{14} \text{ is on} \end{cases} \quad (9)$$

$$S_c = \begin{cases} 1, S_{21} \text{ is on and } S_{22} \text{ is off} \\ 0, S_{21} \text{ is off and } S_{22} \text{ is on} \end{cases} \quad (10)$$

$$S_d = \begin{cases} 1, S_{23} \text{ is on and } S_{24} \text{ is off} \\ 0, S_{23} \text{ is off and } S_{24} \text{ is on} \end{cases} \quad (11)$$

The switching function for the bridge 1 (converter working in buck mode) can be expressed as:

$$S_{bridge1} = S_a - S_b \quad (12)$$

When operating in buck mode, the high frequency transformer receives power from bridge 1. Figure 18 illustrates the DAB converter functioning in the buck mode.

By applying Kirchhoff's voltage law to Bridge 1, the equation of the bridge can be written as follows:

$$L_r \frac{di_L}{dt} = S_{bridge1} V_{in} - nV_{cd} \quad (13)$$

Where:

L_r is the leakage inductance

V_{in} is the voltage at the input, the only source of the system.

When Kirchhoff's current law is used at Bridge 2, the equation of voltage model for the rectifier can be written as follows:

$$C_0 \frac{dV_{out}}{dt} = S_{bridge2} * i_s - i_2 \quad (14)$$

Where:

The output capacitance is C_0

The voltage at the output is V_{out}

The current in the second transformer is i_s

3.4.2 Transfer Function of the DAB

The power transmitted from the bridge 1 to the bridge 2 can be defined as follows (Lucas, Kevin, Pagano, Daniel, Landau, and Renan. (2019)):

$$< P\ (t) >_{T_s} = \frac{< V_{in}(t) >_{T_S} * < V_{out}(t) >_{T_S}}{2\pi f_{sw} L_r} \phi(1-\frac{|\phi|}{\pi}) \qquad (15)$$ (Chen, L., Shao, S., Xiao, Q., Tarisciotti, L., Wheeler, P.W. and Dragičević, T.(2020))

ϕ is the phase shift

f_{sw} denotes the switching frequency

The switching period is expressed as: $T_s = \frac{1}{f_{sw}}$

$< V_{in}(t) >_{T_S}$ is the average switching input voltage

$< V_{out}(t) >_{T_S}$ is the average switching output voltage

V_{ab} and V_{cd} have a square waveform with a duty cycle = 0.5

The difference in phase between V_{ab} and V_{cd} is $\phi(-\frac{\pi}{2} \le \phi \le \frac{\pi}{2})$.

If $\phi > 0$, V_{ab} gets ahead of V_{cd}.

Otherwise, V_{ab} is lagging behind V_{cd}

In this thesis, the unidirectionality of power flow is considered so $\phi > 0$

$$w_{sw} = 2\pi f_{sw}\ , \quad g_m = \frac{1}{\pi w_{sw} L_r} \qquad (16)$$

Substituting (16) into the equation (15)

$$< P(t) >_{T_s} = g_m < V_{in}(t) >_{T_s} < V_{out}(t) >_{T_s} \phi(\pi-\phi) \qquad (17)$$

It is possible to formulate an expression for the transmission power while presuming that the DAB converter performs its function with an efficiency of 100% (i.e., there are no losses).

$$< P(t) >_{T_s} = < V_{in}(t) >_{T_s} * < i_1(t) >_{T_s} = < V_{out}(t) >_{T_s} * < i_2(t) >_{T_s} \qquad (18)$$

$< i_1(t) >_{T_s}$ and $< i_2(t) >_{T_s}$ represent, respectively, the average values of i_1 and i_2 during the course of a switching time.

$< i_1(t) >_{T_s}$ and $< i_2(t) >_{T_s}$ can be defined as:

$$< i_1(t) >_{T_s} = g_m < V_{out}(t) >_{T_s} \phi\ (\pi - \phi) \quad (19)$$

$$< i_2(t) >_{T_s} = g_m < V_{in}(t) >_{T_s} \phi(\pi - \phi) \quad (20)$$

The average value of i_2 is as:

$$< i_2(t) >_{T_s} = C_o \frac{d< V_{out}(t) >_{T_s}}{dt} + \frac{1}{R} < V_{out}(t) >_{T_s} \qquad (21)$$

The variation of average value of V_{out} is:

$$C_o \frac{d < V_{out}(t) >_{T_s}}{dt} = g_m < V_{in}(t) >_{T_s} * \phi\ (\pi - \phi) - \frac{1}{R} < V_{out}(t) >_{T_s} \qquad (22)$$

To obtain a linear model easier to analyze, a small signal model of the system should be constructed. To achieve this, a DC value and a signal component are assigned to each variable as follows:

$$\begin{cases} < i_2(t) >_{T_s} = I_1 + \hat{i}_1(t) \\ \phi = D_\phi + \hat{\phi} \end{cases} \quad (23) \quad \text{and} \quad \begin{cases} < V_{in}(t) >_{T_s} = V_{in} + \hat{V}_{in}(t) \\ < V_{out}(t) >_{T_s} = V_{out} + \hat{V}_{out}(t) \end{cases} \quad (24)$$

I_2, D_ϕ, V_{in} and V_{out} are the DC values

$\hat{V}_{in}(t)$, $\hat{V}_{out}(t)$, $\hat{i}_2(t)$ and $\hat{\phi}$, are the first order ac terms

The equations can be linearized as follows:

$$\begin{cases} \hat{i}_2(s) = G_{sd}\hat{\phi}(s) + G_{sv}(s)\hat{V}_{in}(s) \\ \hat{V}_{out}(s) = Z_{out}\hat{i}_1(s) \end{cases} \quad (25)$$

Where:

$$G_{sd} = \frac{1}{\pi w_{sw} L_r}(\pi - 2D_\phi)V_{in} \quad (26)$$

$$G_{sv} = \frac{1}{\pi w_{sw} L_r} D_\phi(\pi - D_\phi) \quad (27)$$

$$Z_{out} = \frac{R}{1 + sRC_o} \quad (28)$$

Therefore, the DAB's transfer function (small-signal control to output) is defined as:

$$G_{v\phi}(s) = \frac{\hat{V}_{out}(s)}{\hat{\phi}(s)}\bigg|_{\hat{V}_{in}(s)=0} = Z_{out}G_{sd} \quad (29)$$

$$G_{v\phi}(s) = \frac{(\pi - 2D_\phi)}{\pi w_{sw} L_r C_o}\left(\frac{V_{in}}{s + \frac{1}{RC_o}}\right) \quad (30)0$$

CHAPTER 4
CONTROL METHODS OF THE DAB

Closed-loop regulation is required for a DAB converter to its output close to the reference value regardless of the scenarios that might occur, as well as to ensure the reliability of the system (Segaran, D.S. (2013)).

The control of the converter is divided into two (2) tiers:

- The control block is the first part. In the literature, a range of control approaches has been suggested to regulate the DAB converter. In (Segaran, Holmes, D., D.G., McGrath, and B.P. (2008)) the PI control of the DAB is proposed using PSIM simulation. In (Sowmya, Ravichandran and Rama Reddy, S. (2015)) a comparison between PI and Fuzzy logic controlled dual active bridge converter is made. In (Sowmya, Ravichandran and Rama Reddy, S. (2015)), a Moving-Discretized-Control-Set Model-Predictive Control is presented. Several others control methods have been applied in the literature such as fuzzy-neural control, hysteresis control, sliding mode control (Cheng, K.-H., Hsu, C.-F., Lin, C.-M., Lee, T.-T. and Li, C. (2007); Sai, J.-F., Chen, and Y.-P. (2007); Leung, K.-S., K., Chung, and H.S.H. (2005)).

- The modulation block is the second part. Its goal is to control the switches. Single Phase Shift (SPS) modulation (Doncker, R.D., Divan, D. and Kheraluwala, M. (1991)) is by far the most popular type of modulation technique. In this technique, the amount of power that is transmitted is proportionate to the phase shift ϕ. This modulation is ideal for high-power transmission. For low power transfer, other modulation schemes, such as triangular modulation, can be utilized (Zhou, H. and Khambadkone, M. (2009)). In the literature, some researchers suggested a technique combining both methods (Shi, X., Jiang, J. and Guo, X. (2012)).

To summarize, the regulation of the Single-Phase DAB converter can be achieved by the following:

a) Phase shift ϕ: It defines the direction of power flow. Depending on its sign the converter can operate in either forward or reverse mode.

b) Switching duty ratio: Based on the SPS modulation its value is set as 50%. The switching duty ratio is necessary to generate square voltage waveforms for each bridge.

c) Frequency of switches: The switching frequency is a constant that is fixed at a high value in order to minimize the size of the transformer.

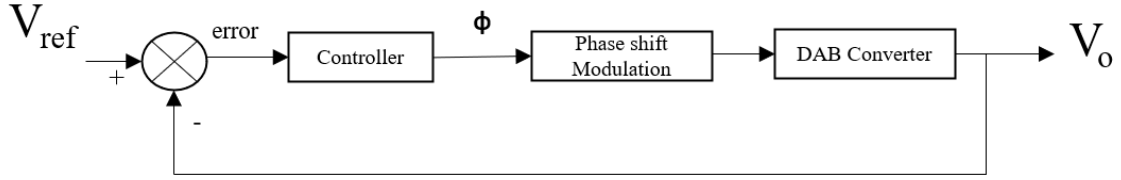

Figure 21: Basic structure of a closed loop control

Figure 21 represents a feedback control of the DAB. First, the reference and the output variable are compared. Based on the error value, the controller takes action accordingly to maintain the output variable as close to the reference.

4.1 PI CONTROL

Since the goal is to control the output voltage, the controller first calculates the difference between the output voltage measured and the set-point. Then by adjusting the process control, the system seeks to reduce or minimize the error, so the voltage value follows the reference.

To increase important performances such as responsiveness of the system, the PI parameters must be tuned according to the application. In the thesis's application, the controller has a feedback signal from the output (secondary bridge) and the reference is a constant value. In comparison to the input voltage, the output voltage increases or decreases proportionally to the set-point error.

The 8 switches are controlled by the conventional PWM generator, and the PI controller generates the phase shift.

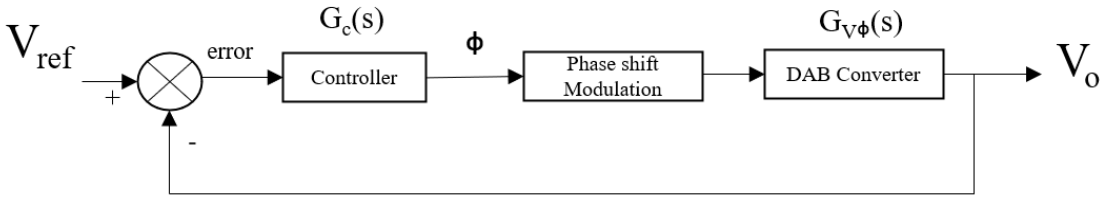

Figure 22: PI Controller Structure

Figure 22 shows the PI control structure of the DAB.

$G_c(s)$ is the transfer function of the controller

$G_{v\phi}(s)$ is the transfer function of the DAB converter

The PI controller generates the phase shift applied to the DAB converter.

4.1.1 PI Transfer Function

The PI controller transfer function is: $G_c(s) = \frac{K_p(s + K_i)}{s}$ (31)

From Figure 22:

$V_o = G_{v\phi}\, G_C\, (V_{ref} - V_o)$ (32)

$V_o(1 + G_{v\phi}\, G_C) = G_{v\phi}\, G_C V_{ref}$ (33)

$$\frac{V_o}{V_{ref}} = \frac{G_{v\phi}\, G_C}{1 + G_{v\phi}\, G_C} \quad (34)$$

$$\frac{V_o(s)}{V_{ref}(s)} = \frac{G_{v\phi}(s)\, G_C(s)}{1 + G_{v\phi}(s)\, G_C(s)} \quad (35)$$

By Substituting the DAB's transfer function expression (30) in (35)

$$G_{v\phi}(s) = \frac{(\pi - 2D_{\phi})}{\pi w_{sw} L_r C_o}\left(\frac{V_{in}}{s + \frac{1}{RC_o}}\right) = \frac{(\pi - 2D_{\phi})}{\pi w_{sw} L_r C_o}\left(\frac{V_{in} RC_o}{1 + RC_o}\right) \quad (36)$$

$$\frac{V_o(s)}{V_{ref}(s)} = \frac{\frac{(\pi - 2D_{\phi})}{\pi w_{sw} L_r C_o}\left(\frac{V_{in} RC_o}{1+RC_o}\right) G_C(s)}{1+\frac{(\pi - 2D_{\phi})}{\pi w_{sw} L_r C_o}\left(\frac{V_{in} RC_o}{1+RC_o}\right) G_C(s)} \quad (37)$$

By Substituting (31) in (37)

$$\frac{V_o(s)}{V_{ref}(s)} = \frac{\frac{(\pi - 2D_{\phi})}{\pi w_{sw} L_r C_o}\left(\frac{V_{in} RC_o}{1+RC_o}\right) \frac{K_p(s + K_i)}{s}}{1+\frac{(\pi - 2D_{\phi})}{\pi w_{sw} L_r C_o}\left(\frac{V_{in} RC_o}{1+RC_o}\right) \frac{K_p(s + K_i)}{s}} \quad (39)$$

(39) is the PI transfer function of the whole system.

4.2 Model Predictive Control of the DAB Converter

MPC can be defined as an advanced control strategy used to control a system while taking the constraints into account. Using the mathematical system's model, the MPC generates predictions regarding the future behavior of the plant. Modelling is a key aspect of the MPC design process since it represents the system's core.

Put simply, MPC is a powerful optimization strategy relying on the model of the plant for feedback control. In order to establish the most effective control action for bringing the output voltage closer to the reference, it employs an online optimization method.

MPC has the capability of incorporating future actions into the control algorithm, which boosts controller performance. Different groups of predictive control methods can be classified in Figure 23.

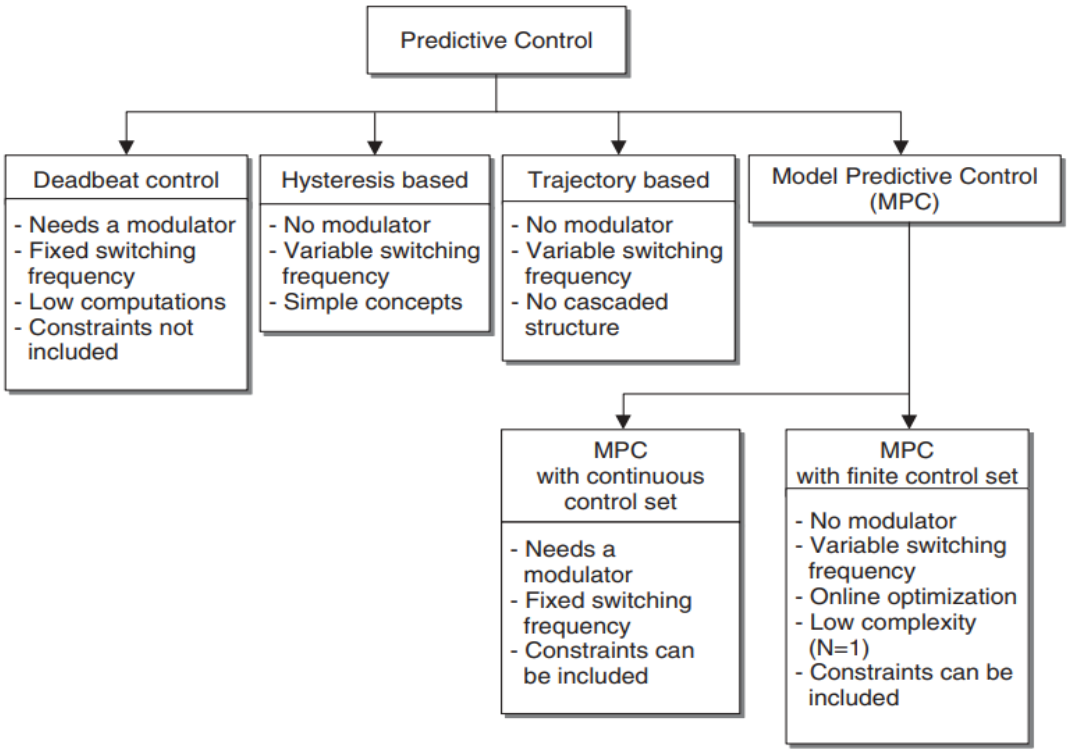

Figure 23: Predictive control approaches (Cortes et al., 2008 © IEEE)

4.2.1 Basics of MPC

MPC was largely used in industry in the past: chemical process industry particularly. Nowadays, this control method is being integrated into power electronics systems. The general idea of MPC was developed in the 1960s.

In power electronics, the very first uses of MPC may be traced all the way back to the early 1980s (Zeng, Jianwu, Du, Xia, Yang and Zhaoxia. (2021)). Because of the significant amount of computation time that is necessary for the control algorithm, it was not conceivable at that time to make advantage of greater switching frequencies. However, in the past ten years, due to advancements in scientific research as well as the

development of potent microprocessors, the utilization of the MPC has become conceivable in a variety of applications within the field of power electronics.

The MPC has several significant advantages:

- Straightforward formulation
- Manages constraints
- Compared to competing for advanced control methods, development time is substantially less.
- Changing the model is easier to maintain because it does not always necessitate a complete redesign.

However, as compared to traditional controllers, the MPC has several drawbacks, such as a higher number of calculations. The quality of the model influences controller, so in the event that the parameters of the system vary over the course of time, it is necessary to take into consideration some adjustment.

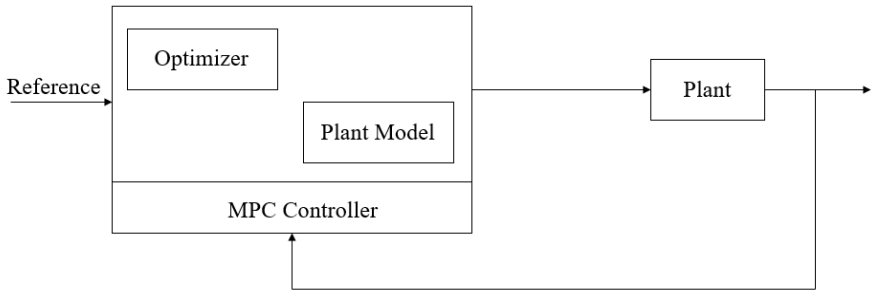

Figure 24: Basic Structure of MPC

Figure 24 depicts the MPC general structure. The MPC controller minimizes the difference between the reference and predicted output value in the system by consistently resolving an optimization control problem while satisfying constraints. The MPC controller's goal is to find the best-predicted action that brings the output value as close to the reference.

To summarize, the most fundamental concepts covered in MPC are:

• The use of the plant's model

• The optimization of a cost function.

The Figure 25 shows the model predictive control strategy.

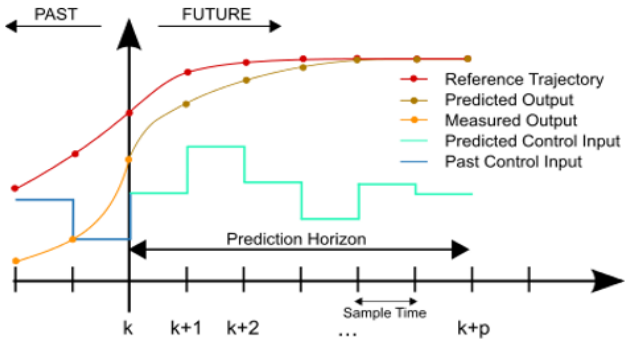

Figure 25: MPC Strategy

Note: Image from Wikipedia https://en.wikipedia.org/wiki/File:MPC_scheme_basic.svg

4.2.2 Predictive Control of the Single-Phase DAB

This thesis aims to control DAB converter output voltage using MPC. Knowing that the DAB Converter is bidirectional in power flow, we assume that the input battery is the only power source. The DAB Converter output voltage is controlled using moving discretized model predictive control. The Single-Phase Shift is used to generate the required voltages. The system operates at a fixed switching frequency and no constraint has been included.

4.2.3 Control Strategy of the DAB Using MPC

The MPC method operates according to different switching states, the phase shift existing between the two bridges, and the leakage inductance L_r which allows the power transfer. A selection criterion with a cost function that evaluates the marge between the reference value of the voltage and the predicted values must be defined for the proper switching state.

The prior steps to design the MPC for a DAB converter are as followed:

• Writing the mathematical model of the converter

• Defining an algorithm for prediction

• Defining a cost function g

4.2.4 Model of the DAB Converter Supplying a Load R

For the DAB converter, there are several modelling techniques, including:

- The Reduced order model
- The Improved reduced order
- The Generalized average model
- The Discrete-time model

4.2.4.1 Reduced Order Model

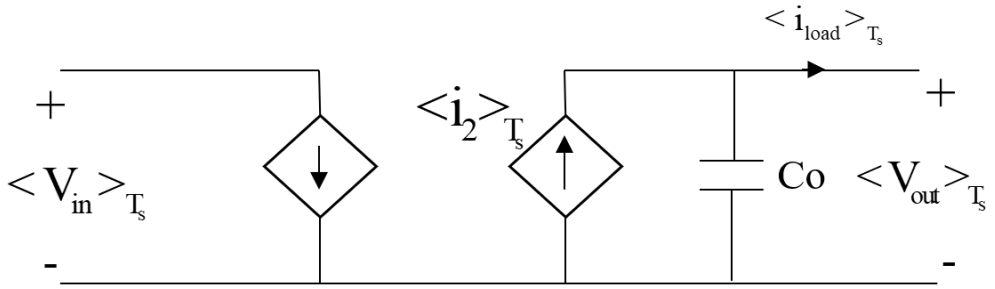

Figure 26: DAB model average

The Figure 26 presents a reduced-order-model of the plant. T_s denotes one switching period. For transmitting power from the Bridge 1 to the load, a phase shift ($D_\phi T_s$) is controlled.

From the model in Figure 26:

$$< i_2 >_{Ts} = \frac{V_{in}}{f_{sw} L_r} D_\phi (1 - 2D_\phi) \qquad (40)$$

As the primary function of the controller is to regulate the output voltage V_{out}, the following dynamic equation describes the output voltage equation:

$$C_o \frac{d < V_{out} >}{dt} = < i_2 >_{T_s} - < i_{load} >_{T_s} \qquad (41)$$

4.2.4.2 Discrete-Time Model

This model predicts next sample interval (k+1) voltage values. The predictive function is obtained using Euler's forward method:

$$\frac{d_y}{d_t} \approx \frac{y(k+1) - y(k)}{T_s} \qquad (42)$$

$$< V_{out}(k+1) > = \frac{i_2(k) - i_{load}(k)}{C_o * f_{sw}} + V_{out}(k) \qquad (43)$$

Assuming that there is not a significant amount of variation in the load current throughout a sampling period

$$I_{load}(k) = I_{load}(k+1) \qquad (37)$$

At $k+2$, the output voltage prediction is:

$$< V_{out}(k+2) > = \frac{i_2(k+1) - i_{load}(k)}{C_o * f_{sw}} + V_{out}(k+1) \qquad (44)$$

By substitution:

$$< V_{out}(k+2) > = \frac{i_2(k+1) + i_2(k) - 2I_{load}(k)}{C_o * f_{sw}} + V_{out}(k) \qquad (45)$$

$$< V_{out}(k+1) > = \frac{V_{in}(k) * D_{\phi}(1 - 2D_{\phi})}{L_r * f_{sw}} \left(\frac{Ts}{C_o}\right) - i_{load}(k) + V_{out}(k) \qquad (46)$$

4.2.5 Cost Function

The objective is to bring the measured output voltage as close as possible to the reference. The cost function in this system is used to calculate the voltage difference that exists between the reference and the predicted voltage values:

$$g = (V_{out\_ref} - V_{out}(k+1))^2 \qquad (47)$$

Where:

V_{out_ref} is the reference value of the voltage

$V_{out}(k+1)$ is the predictive value of the voltage

g is the cost function

4.2.6 Moving Discretized Control Set MPC of DAB Converter

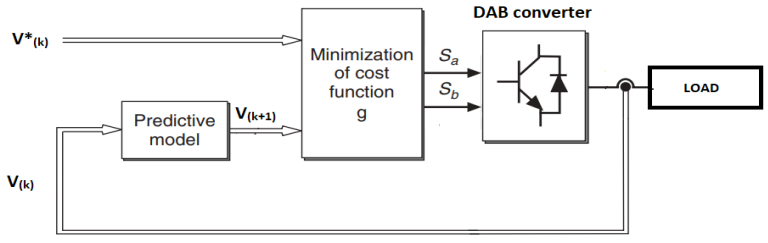

Figure 27: Predictive Voltage control block diagram

Figure 27 shows a block schematic of a predictive control technique for voltage regulation in a DAB Converter. A cost function compares the output variable with the

reference. According to the result obtained, the algorithm generates and applies the required phase shift between the converter's bridges to allow the power transfer while maintaining the output voltage close to the reference.

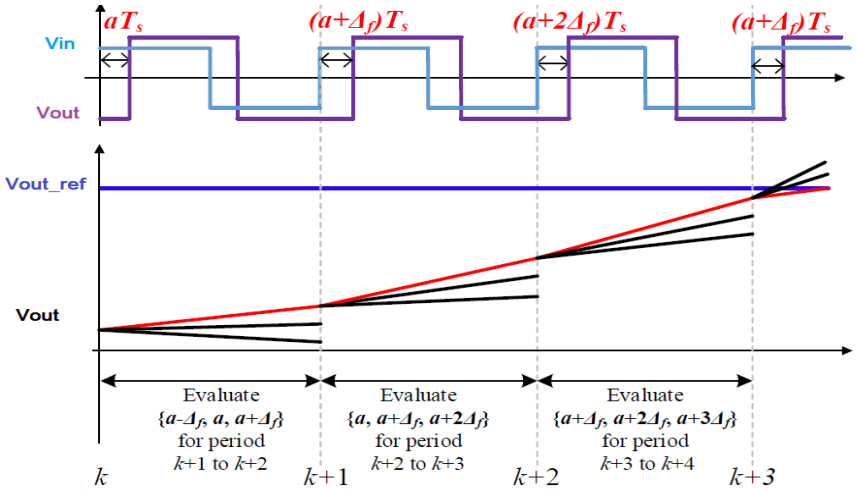

Figure 28: Operating principle of the MPC for DAB

Note: Image from Chen, L., Shao, S., Xiao, Q., Tarisciotti, L., Wheeler, P.W. and Dragičević, T.(2020)

Figure 28 depicts the intuitive mechanism of the MDCMPC DAB Converter. D_ϕ is a continuous variable. Δf represents the phase shift value with the highest level of precision.

The DAB functions properly for one-way power flow (from bridge 1 to bridge 2) under the following parameters of D_ϕ :

$$D_\phi \in [0, 0.5] \quad (48)$$

$$D_\phi \in \{0, \Delta f, 2\Delta f, \ldots 0.5\} \quad (49)$$

4.2.9 Cost Function Proposed

The proposed cost function can be represented as follows:

$$g = G_a + G_b \quad (50)$$

$$\begin{cases} G_a = (V_{out\_ref} - V_{out}(k+1))^2 \\ G_b = (V_{out}(k+1) - V_{out}(k))^2 \end{cases} \quad (51)$$

In this expression, the first term G_a oversees regulating the voltage V_{out} to the set-point value V_{out_ref}. The second term G_b, oversees reducing voltage divergence. G_a plays an important role in the cost function expression when Vout gets far from the reference value. When Vout gets close to the output voltage reference value V_{out_ref}, G_b come into effect and minimizes the fluctuation over the set point. Put simply, the goal of G_b is to limit the variation of the voltage value over the reference value.

CHAPTER 5

SIMULATIONS RESULTS

This chapter presents the simulation's results of the Single-Phase DAB converter controlled by using the PI controller and the model predictive control method. Firstly, the parameter settings are given then the performances of the bidirectional converter under different conditions are presented. The fundamentals parameters used in the Matlab Smulink model are given in Table 2.

The capacitor C_o is set at a large value to filter the output voltage ripple. The leakage inductance L is also set at a large value to allow the power transfer between the two bridges. The input voltage can be modulated manually to dynamically analyze the influence of a disturbance at the input voltage on the other variables of the system. The operating characteristics of the components in DAB converter for Simulation are given in Table 2, these parameters are depicted from the literature and are the most common parameters used for operation.

Table 2: Operating parameters for simulation

Parameters	**Values**
Converter rated power P	650 W
Primary voltage Vin	100 V
Secondary Voltage Vout	70 V
Transformer turn ration n	1
Power transfer inductance L_r	280 µH
Switching frequency f_{sw}	5 kHz
Load resistor R	20 Ω
Capacitance C_o	10000 µF

5.1 PI Control of DAB converter

After the design of the PI controller, the parameters are implemented in Simulink for simulation. Figure 29 depicts the circuit of the DAB converter supplying power to the load R. Power flows from the bridge 1 to the bridge 2 of the circuit.

The variable time delay block and the pulse generator block are used to generate the voltages Vab and Vcd. The PI controller generates the phase shift required to allow the power transfer. The pulses generated by the pulse generator block are 50% and the frequency is constant.

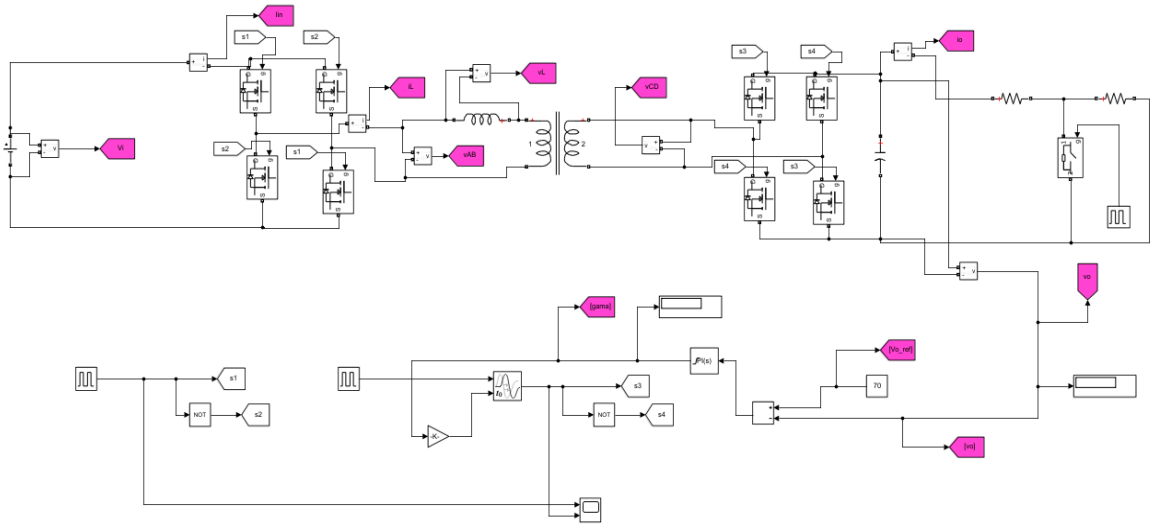

Figure 29: Circuit diagram of the PI control of the DAB converter

The PI controller is tuned manually. In this tuning method, Ki and Kp are set to zero

The tuning of the PI controller used in this thesis is made is three steps:

- Firstly, the Kp value is increased gradually until the output of the loop oscillates at constant amplitude.

- Secondly, the Kp value is then set to half of its value and adjusted. The Kp value found for the system is: 0.0012

- Thirdly, the Ki value is increased until overshoot is minimized. In fact if the Ki value is too high, this would cause instability of the system

The Ki value for the system is: 1e-4

Therefore, for all the simulation made with PI controller in this thesis: Kp = 0.0012 and Ki=1e-4.

5.1.1 Voltage waveform

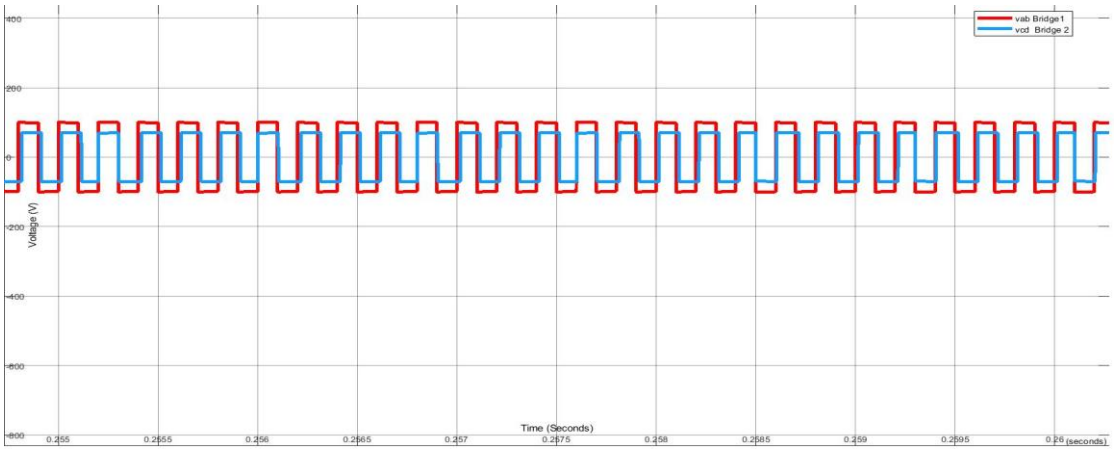

Figure 30: SPS voltage waveforms

Figure 30 depicts the phase shifted voltages waveforms. As the system operates in forward mode, Vab is ahead of Vcd

5.1.2 Simulation Results: Stable Load R

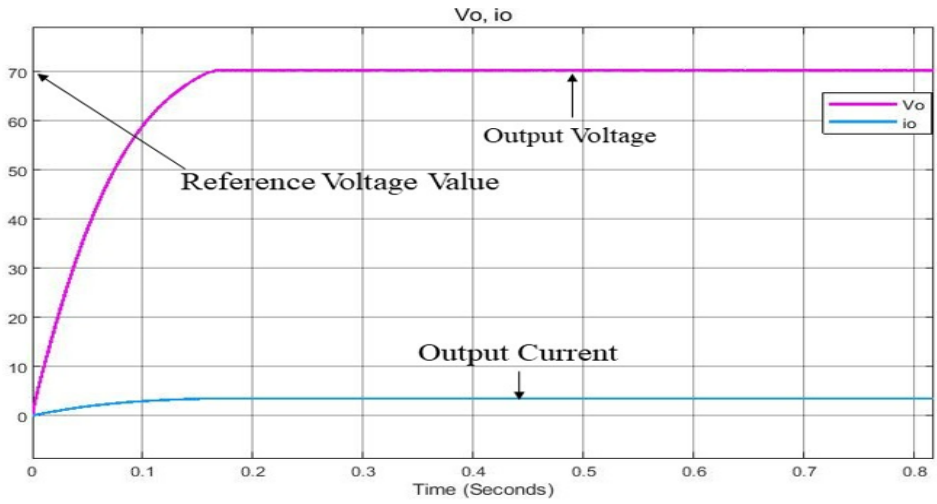

Figure 31: Output voltage and Output Current

The voltage and current at the output of the DAB after simulation are shown in Figure 31. The output current is 3.51 Amps, and the output voltage is 70V. The response reaches the set-point at t=0.163s. Then the output voltage follows the reference value V=70V accurately during the operation of the system.

5.1.3 Simulation Results: Variation in the Load (Dynamic Response)

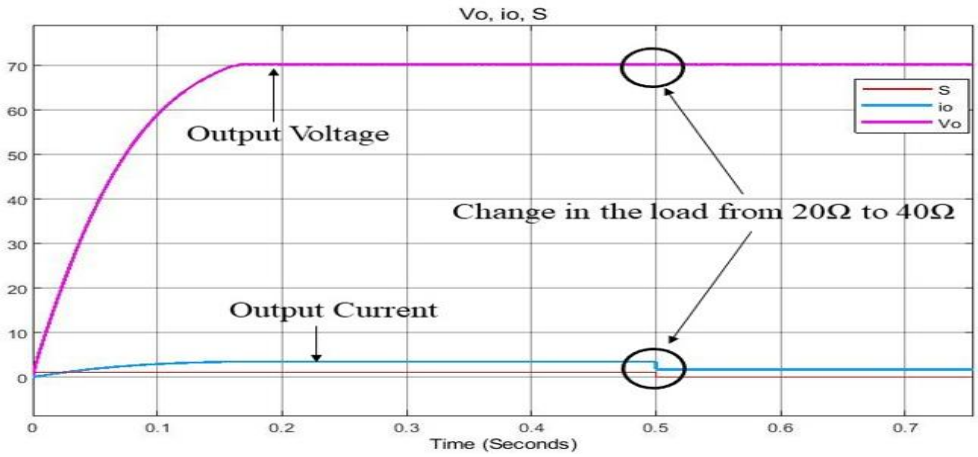

Figure 32: Step change of the load

Figure 32 shows the waveforms of the output voltage and current when the load changes suddenly. To vary the load during the simulation, an ideal switch controlled by a pulse generator and two resistors connected in series are used as depicted on the Figure 33.

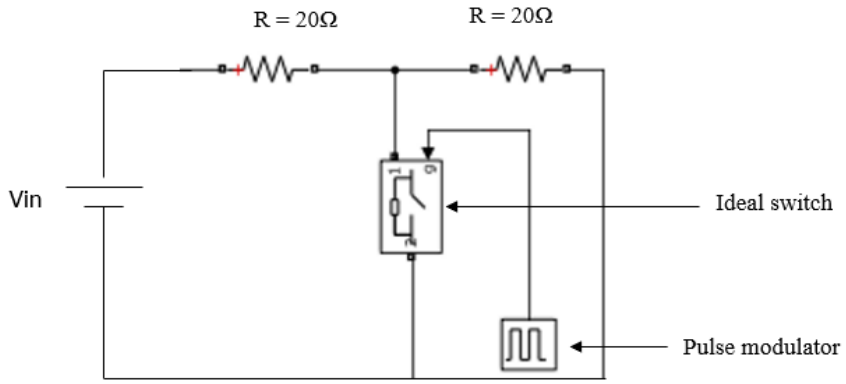

Figure 33: Variable load

In Figure 33, the pulse generator the period is set as 1 second and the pulse width 50%. This way the switch will be ON for 0.5 seconds so the load will be 20Ω then will change to its double value: 40Ω.

The results obtained in Figure 32 show that at t=0.5s the load increases from 20 ohm to 40 ohm. The PI has a good response and meets the control requirements showing an interesting dynamic performance while facing a disturbance at the load (sudden variation).

5.1.4 Simulation Results: Variation in Vin (Disturbance)

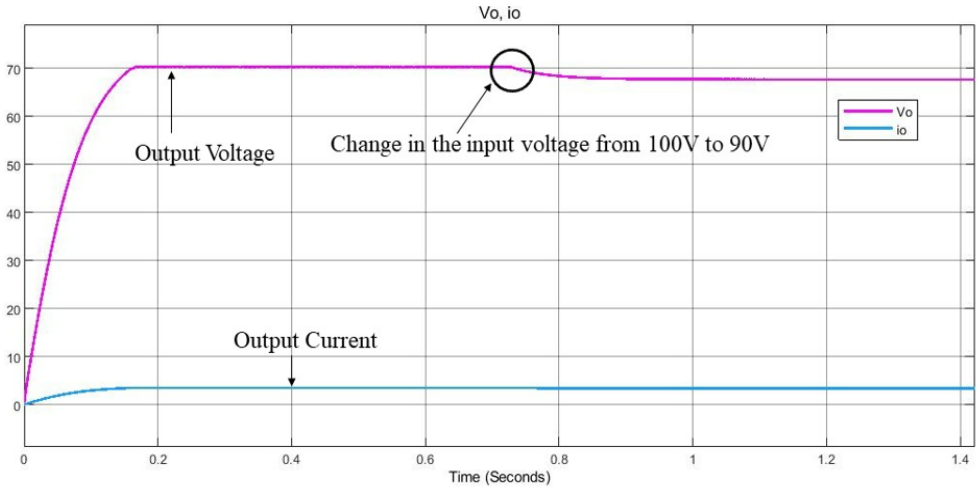

Figure 34: Change in the input Voltage (Disturbance)

The response to a change in the input voltage from 100V to 90V is depicted in Figure 34. When the voltage changes from 100V to 90V, the output voltage deviates from the reference and does not get back to the initial value. The disturbance influences the system which becomes unstable. The output voltage shows a significant steady-state error.

In the application, it is required to build a control strategy that maintains the system's stability regardless of any input-side disturbances. In order to meet the new requirement when facing a change of input voltage, the controller must be redesigned.

5.2 MPC Control of DAB converter

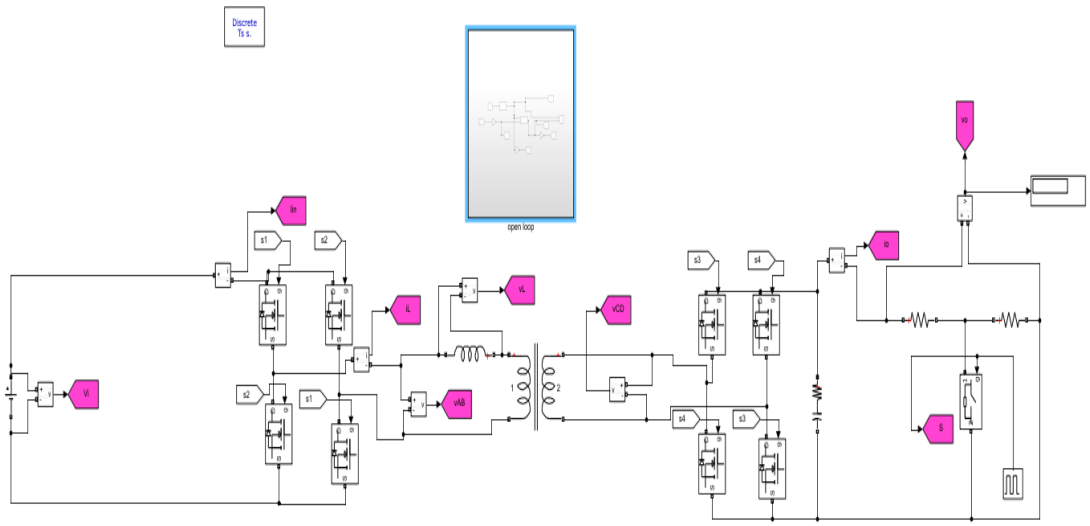

Figure 35: Circuit diagram of the MPC of the DAB converter

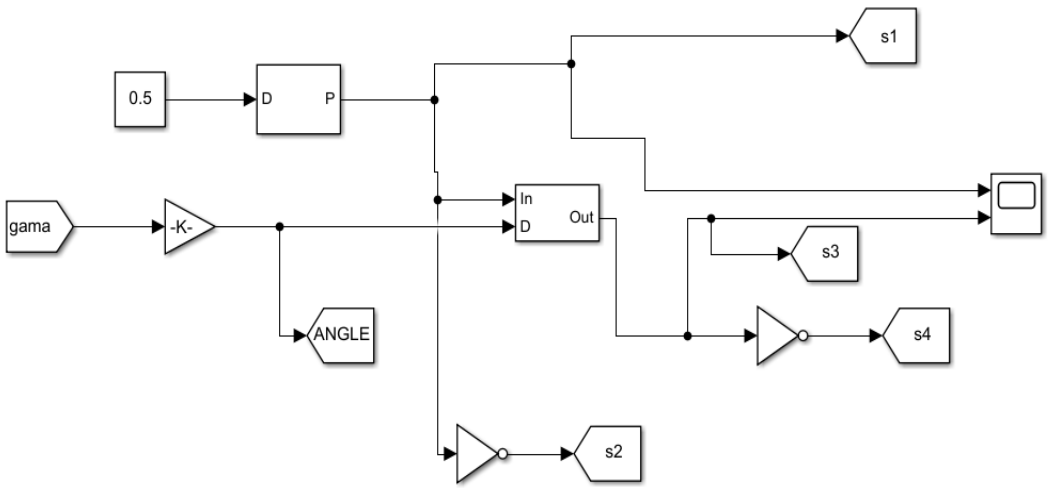

Figure 36: Pulses generator for the switches

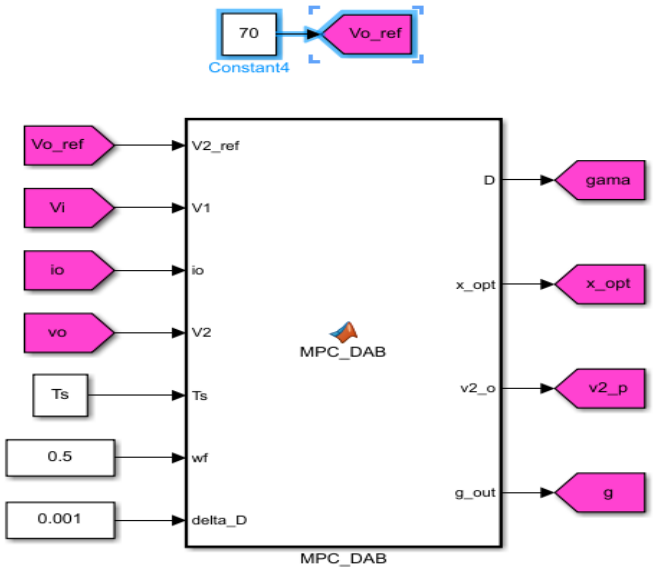

Figure 37: Block containing the control algorithm

5.2.1 Voltage Waveform

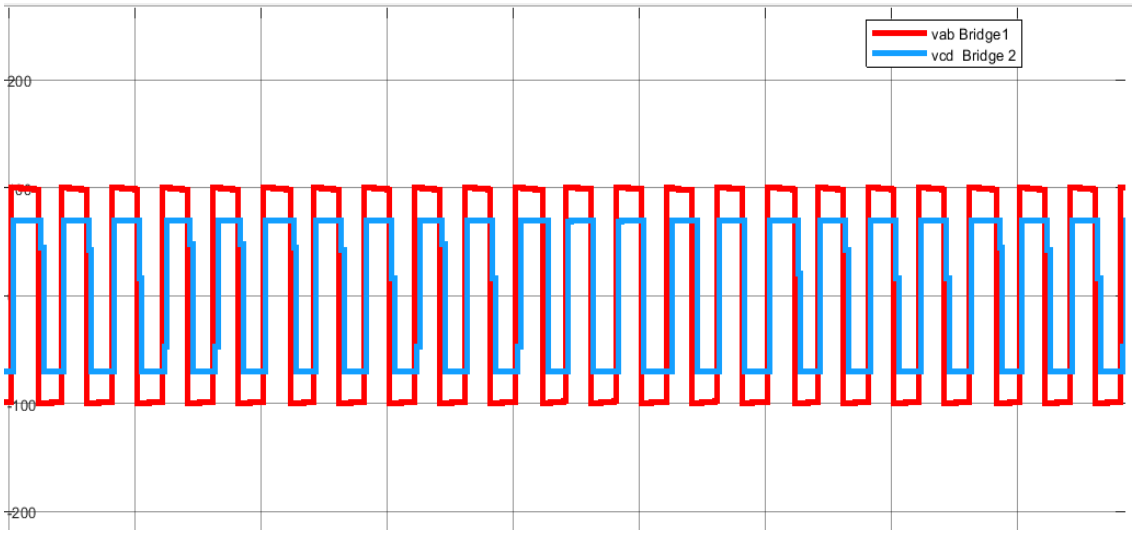

Figure 38: SPS voltage waveforms

Figure 38 depicts the phase shifted voltages waveforms. Vab is phase shifted from Vcd. In the operation of the Dual active bridge converter with SPS modulation technique there should be a phase shift to transfer the power between the bridges.

5.2.2 Simulation Results: Stable Load R

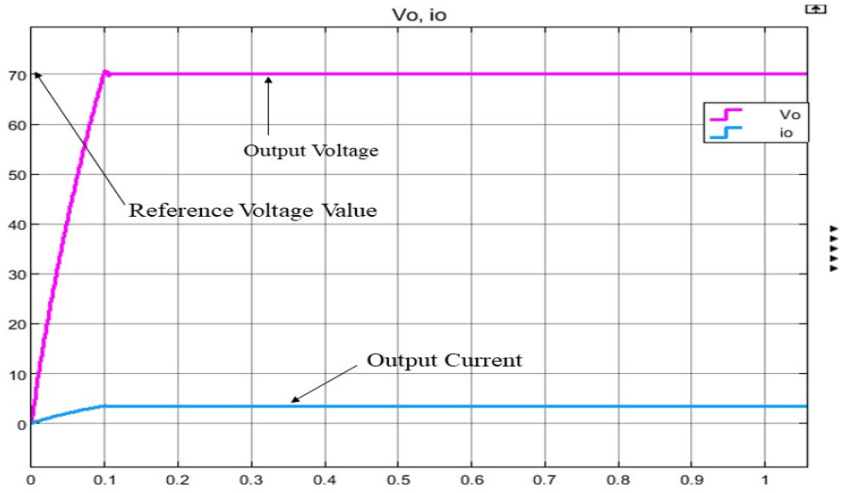

Figure 39: Output voltage and Output Current

Figure 39 illustrates the output voltage as well as the output current. The current at the output is 3.51 A, and the output voltage is 70 V. The results reveals that the response reaches the set point very fast (at t=0.099s). The output voltage follows the reference value V=70V accurately during the operation of the system.

5.2.3 Simulation Results: Variation in the Load (Dynamic Response)

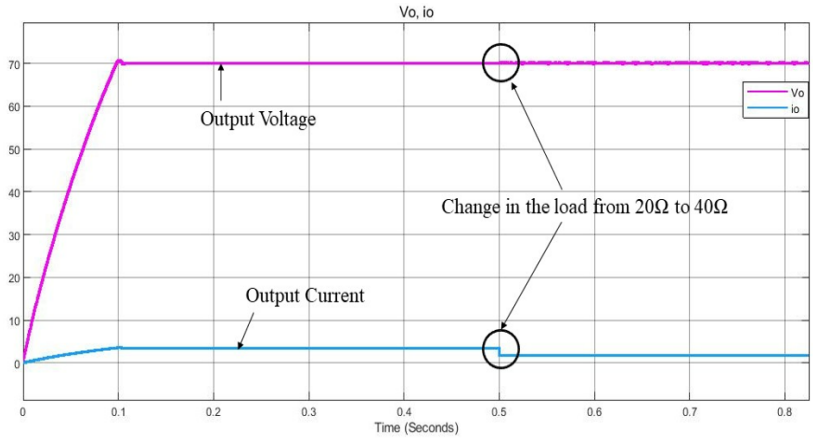

Figure 40: Step change of the load

Figure 40 depicts the response to step change in the load at t=05s. At t=0.5s the load changes from 20 ohm to 40 ohm. The fluctuation is observed due to the power variation. The overshoot is not significant due to the fast response of the MPC. MPC enables the convergence of the output voltage value to the desired reference. The results reveal that the model predictive control meets the control requirements and show an interesting dynamic performance while facing a disturbance at the load (sudden variation).

5.2.4 Simulation Results: Variation in Vin (Disturbance)

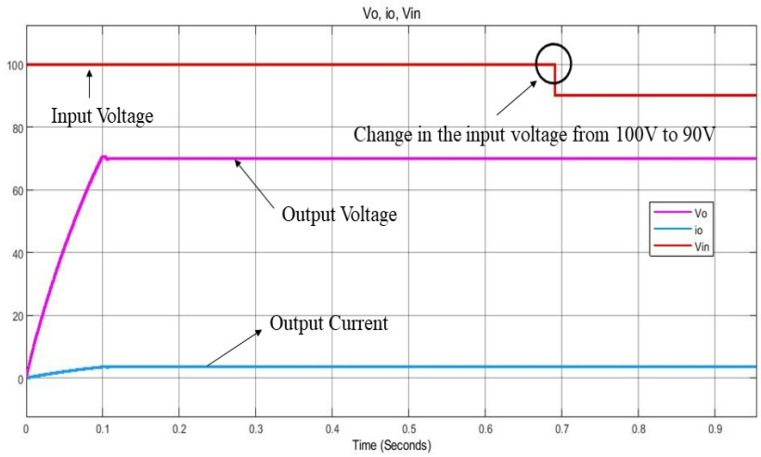

Figure 41: Step change of the input Voltage (Disturbance)

The response to a step change in the input voltage from 100V to 90V is depicted in Figure 41. With the control approach used, there are almost no variations in the output voltage, and there is no fluctuation despite changes in the input voltage.

The results show that the model predictive control meets the control requirements and has a dynamic performance that is intriguing when integrating the disturbance at the input voltage. The MPC shows good disturbance rejection properties and increases system robustness.

5.2.5 Cost Function

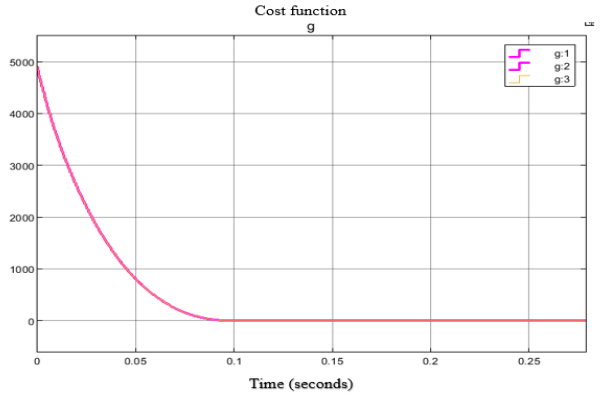

Figure 42: Cost function

The cost function of the system is depicted in the Figure 42. The error turns to 0 in 0.09 seconds. This is due to the fast responsiveness of the MPC.

5.3 Comparison Between the PI and MPC

The comparison of reaction with PI and MPC are summarized in the tables 3, 4 and 5.

Table 3: Comparison of PI and MPC at Stable Load

Type of Controllers	Settling time (seconds)	Peak time (seconds)	Overshoot (%) (seconds)	Steady state error (volts)
PI Controller	0.163	0.186	0.962	0.3
MPC	0.099	0.102	2.941	0.001

From Table 3, when operating under stable load condition, the MPC has a quicker response (at t=s0.099s), whereas the PI control approach has a lower responsiveness. PI has a lower overshoot than MPC, but its steady-state error is significantly higher. With the MPC, the output variable gets to the peak time in a short amount of time compared to the PI.

Table 4: Comparison of PI and MPC with Step change in the load at t=0.5 seconds

Type of Controllers	Settling time (seconds)	Peak time (seconds)	Overshoot (%) (seconds)	Steady state error (volts)
PI Controller	0.163	0.535	0.982	0.32
MPC	0.099	0.102	0.962	0.2

The results in Table 4 reveal that, when operating with a step change in the load, the MPC still demonstrates a faster response, in addition to presenting a lower steady state error and overshoot. The PI gets to the peak time a little bit later than the MPC.

Table 5: Comparison of PI and MPC with Step change in the input voltage

Type of Controllers	Settling time (seconds)	Overshoot (%) (seconds)	Steady state error (volts)
PI Controller	0.163	7.143	2.62
MPC	0.099	2.941	0.12

The results obtained in Table 5 demonstrate the reliability and robustness of the MPC. While the system working with PI becomes completely unstable due to the change in the input voltage, the system working with MPC maintains its stability by presenting a faster response, lower overshoot, and steady state error.

CHAPTER 6
CONCLUSION AND WORK TO BE DONE IN THE FUTURE

6.1 Conclusion

A comparative study of the PI with MPC control is done in this thesis. Closed-loop controlled PI and MPC controlled DAB DC to DC converters are designed and simulated successfully using MATLAB. Their responses are compared. The results indicate that the MPC-controlled converter has a faster response and minimum steady-state error in the output. With the step change in the input voltage, the PI controller's parameters need to be redesigned to reach stability while the MPC has a better response to disturbance. The MPC controller has advantages like improved efficiency, robustness, and good transient response. Based on the overall results, the MPC response is superior to the PI-controlled system. Therefore, the MPC control is the best control method to choose for the system operation. The disadvantage of this converter is that it requires a high algorithm complexity.

6.2 Future Work

Future work should consider the losses generated by the transformer and other components. To determine the transformer's losses, the design of the transformer, its material qualities, and dimensions, as well as copper and coil losses, must be considered.

This thesis only studied the unidirectionality of power flow. Hence, the Boost operation of the converter needs to be investigated and analyzed. In future work, a battery should be considered at the output. To verify the MATLAB Simulation results, a prototype of a DAB converter connected to a load should be built. The prototype design will contain two parts which are the Hardware design and the Software design.

REFERENCES

Articles

W. N. A. Report. Comparison of Lifecycle Greenhouse Gas Emissions of Various Electricity Generation Sources. *World Nucl. Assoc., p. 10, 2011.*

Zeng, Jianwu, Du, Xia, Yang. and Zhaoxia. (2021). A Multiport Bidirectional DC-DC Converter for Hybrid Renewable Energy System Integration. *IEEE Transactions on Power Electronics. PP. 1-1. 10.1109/TPEL.2021.3082427.*

Zhao, B., Song, Q., Liu, W. and Sun, Y. (2014). Overview of dual-active-bridge isolated bidirectional dc–dc converter for high-frequency-link power-conversion system. *IEEE Transactions on Power Electronics, vol. 29, no. 8, pp. 4091–4106.*

Naayagi, R., Forsyth, A.J. and Shuttleworth, R. (2012). High-power bidirectional dc–dc converter for aerospace applications. *IEEE Transactions on Power Electronics, vol. 27, no. 11, pp. 4366–4379,.*

Harrye, Y.A., Ahmed, K.H., Adam, G.P. and Aboushady, A.A. (2014). Comprehensive steady state analysis of bidirectional dual active bridge DC/DC converter using triple phase shift control. *IEEE 23rd International Symposium on Industrial Electronics (ISIE), pp. 437-442, doi: 10.1109/ISIE.2014.6864653.*

Abraham, Y.H., Wen, H., Xiao, W. and Khadkikar, V. (2011). Estimating power losses in Dual Active Bridge DC-DC converter. *2nd Int. Conf. Electr. Power Energy Convers. Syst. EPECS 2011, pp. 1–5, 2011, doi: 10.1109/EPECS.2011.6126790.*

Kayaalp, İlker, Demirdelen, Tuğçe, Tümay. and Mehmet. (2016). A Novel Fuzzy Logic Control for Bidirectional DC-DC Converter and Comparison with Dual Phase-Shift Control Method in Medium Voltage Applications. *10.1109/CIVEMSA.2016.7524324.*

Doncker, R.D., Divan, D. and Kheraluwala, M. (1991). A three-phase soft switched high-power-density dc/dc converter for high-power application. *IEEE TRANSACTIONS ON INDUSTRY APPLICATION, vol. 27, no. 1, pp. 63–73, January/February 1991.*

Segaran, D.S. (2013). Dynamic modelling and control of dual active bridge bi-directional dc-dc converters for smart grid applications. (2013). *Ph.D. dissertation,*

school of Electrical and Computer Engineering (SECE) RMIT University, February 2013

Segaran, Holmes, D., D.G., McGrath. and B.P. (2008). Comparative analysis of single and three-phase dual active bridge bidirectional dc-dc converters. *Australian Universities Power Engineering Conference, pp. 1–6, December 2008.*

Sowmya, Ravichandran. and Rama Reddy, S. (2015). Comparison of PI & Fuzzy Logic Controlled Dual Active Bridge DC to DC Converter Systems.

Chen, L., Shao, S., Xiao, Q., Tarisciotti, L., Wheeler, P.W. and Dragičević, T.(2020). Model Predictive Control for Dual-Active-Bridge Converters Supplying Pulsed Power Loads in Naval DC Micro-Grids. *IEEE Transactions on Power Electronics, vol. 35, no. 2, pp. 1957-1966, Feb. 2020, doi: 10.1109/TPEL.2019.2917450.*

Zhou, H. and Khambadkone, M. (2009). Hybrid modulation for dual active bridge bidirectional converter with extended power range for ultracapacitor application. *IEEE TRANSACTIONS ON INDUSTRY APPLICATION, vol. 45, no. 4, pp. 1434–1442, July 2009*

Lucas, Kevin, Pagano, Daniel, Landau. and Renan. (2019). Single Phase-Shift Control of DAB Converter using Robust Parametric Approach. *1-6. 10.1109/COBEP/SPEC44138.2019.9065902.*

Gang, C., Yim-Shu, L., Hui, S.Y.R., Xu, D. and Wang, Y. (2000). Actively clamped bidirectional flyback converter. *IEEE Trans. Ind. Electron., vol. 47, no. 4, pp. 770--779, 2000.*

Cacciato, M., Caricchi, F., Giuhlii, F. and Santini, E. (2004). A critical evaluation and design of bi-directional dc/dc converters for super-capacitors interfacing in fuel cell applications. *Proc. 39th IEEE Industry Applications Society Annual Meeting (IAS), vol. 2, 2004, pp. 1127--1133.*

R. W. A. A., De Doncker, Divan, D.M. and Kheraluwala, M. H. (1993). A three-phase soft-switched high-power-density dc-dc converter for high-power applications. *IEEE Trans. Ind. Appl., vol. 27, no. 1, pp. 63--73, 1991, 0093-9994.*

Yade, Ousseynou, Gauthier, Jean-Yves, lin shi, Xuefang, Gendrin, Martin, Zaoui. and Abderrahim. (2015). Modulation strategy for a Dual Active Bridge converter using Model Predictive Control. *15-20. 10.1109/PRECEDE.2015.7395578.*

Shi, X., Jiang, J. and Guo, X. (2012). An efficiency-optimized isolated bidirectional dc-dc converter with extended power ranger for energy storage systems in microgrids. *Energy, vol. 6, pp. 27–44, 2012.*

R. W. A. A., De Doncker, Divan, D. M. and Kheraluwala, M. H. (1991). A Three-Phase SoftSwitched High-Power-Density DC/DC Converter for High-Power Applications. *IEEE Trans. Ind. Appl., vol. 27, no. 1, pp. 63–73, 1991.*

Krismer, F. and Kolar, J.W. (2010). Accurate power loss model derivation of a high-current dual active bridge converter for an automotive application. *IEEE Trans. Ind. Electron., vol. 57, no. 3, pp. 881–891, 2010*

Tsai, M.T., Chu, C.L., Yang, Y.Z. and Wu, D. R. (2016). Design of a Dual Active Bridge DC-DC Converter for Photovoltaic System Application. *I. E. Letters (2016) vol. 7, no. 8, pp. 1805– 1812, 2016*

Barone, G., Brusco, G., Burgio, A., Menniti, D., Pinnarelli, A. and Sorrentino, N. (2014). A power management and control strategy with grid-ancillary services for a microgrid based on DC bus. *Int. Rev. Electr. Eng., vol. 9, no. 4, pp. 792–802, 2014.*

Cheng, K.-H., Hsu, C.-F., Lin, C.-M., Lee, T.-T. and Li, C. (2007). Fuzzy–neural sliding-mode control for DC–DC converters using asymmetric Gaussian membership functions. *IEEE Trans. Ind. Electron., 54(3), 1528-1536.*

Sai, J.-F., Chen. and Y.-P. (2007). Sliding mode control and stability analysis of buck DC-DC converter. *International Journal of Electronics, 94(3), 209-222.*

Leung, K.-S., K., Chung. and H.S.H. (2005). Dynamic hysteresis band control of the buck converter with fast transient response. *IEEE Trans. Circuits Syst., 52(7), 398-402.*

Appendix 1: MATLAB PLOTS WITH PI CONTROLLER

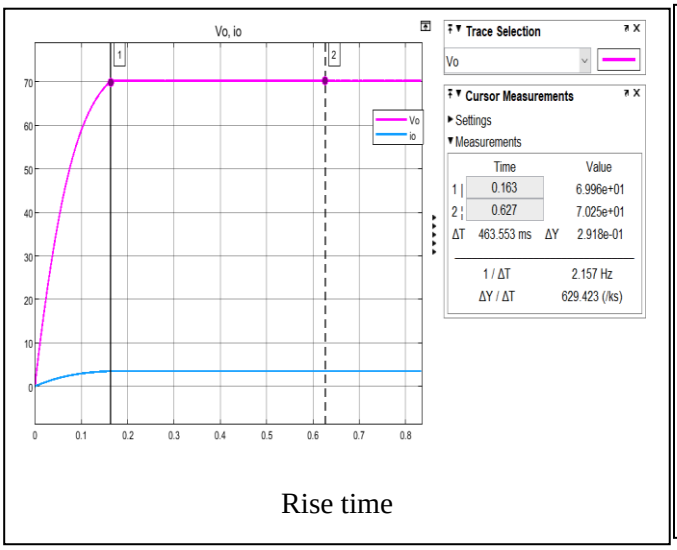

Rise time

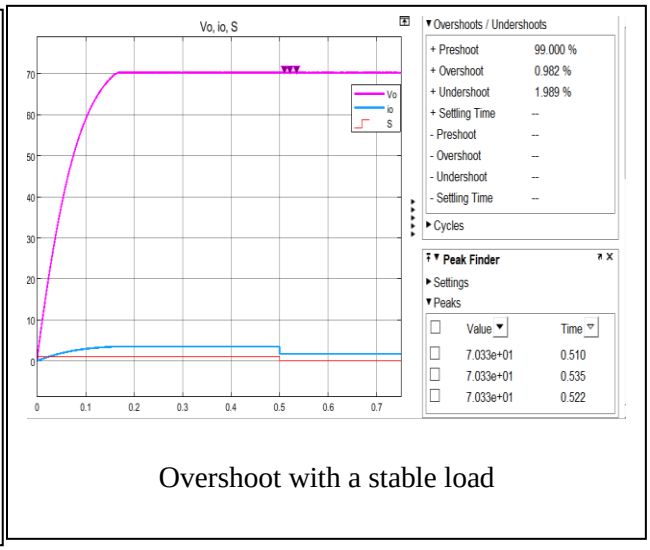

Overshoot with a stable load

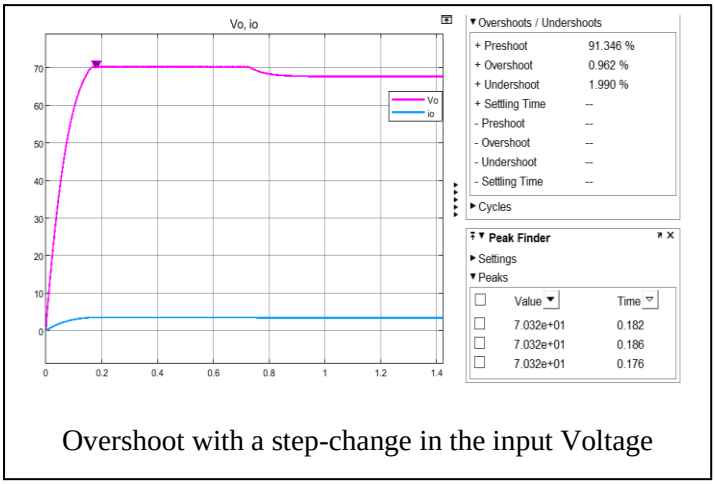

Overshoot with a step-change in the input Voltage

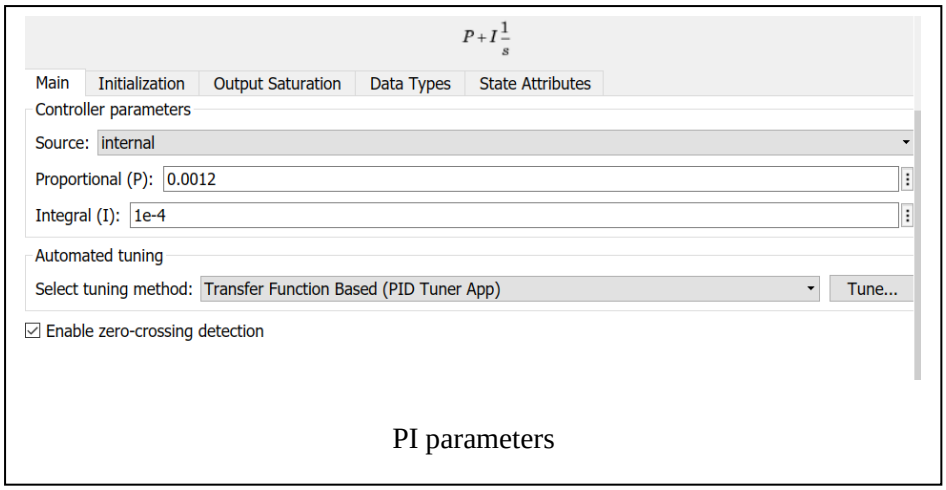

PI parameters

Appendix 2: MATLAB PLOTS WITH MPC

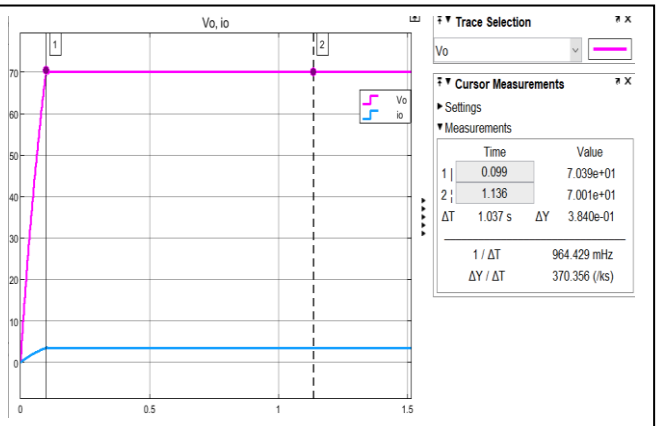

Rise time

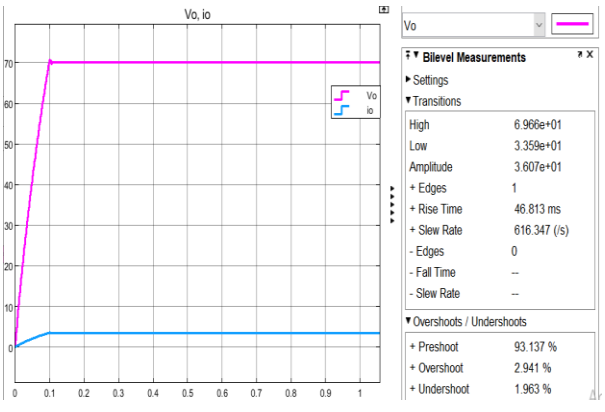

Overshoot with a stable load

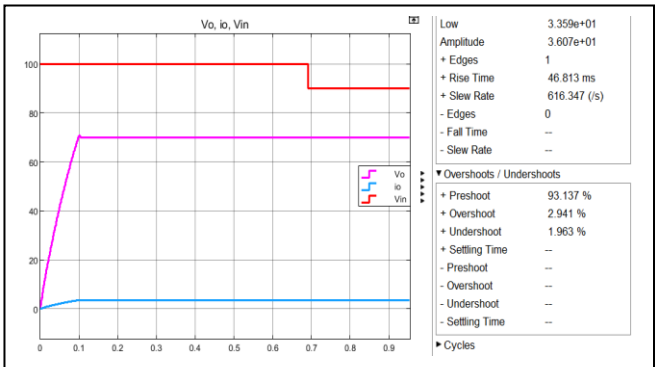

Overshoot with a step change in the input Voltage

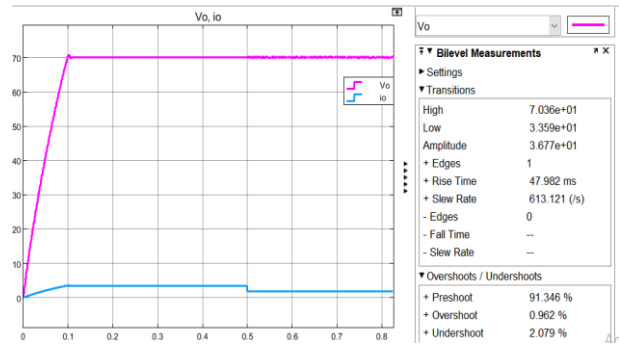

Overshoot with a step-change in the load at t=0.5s